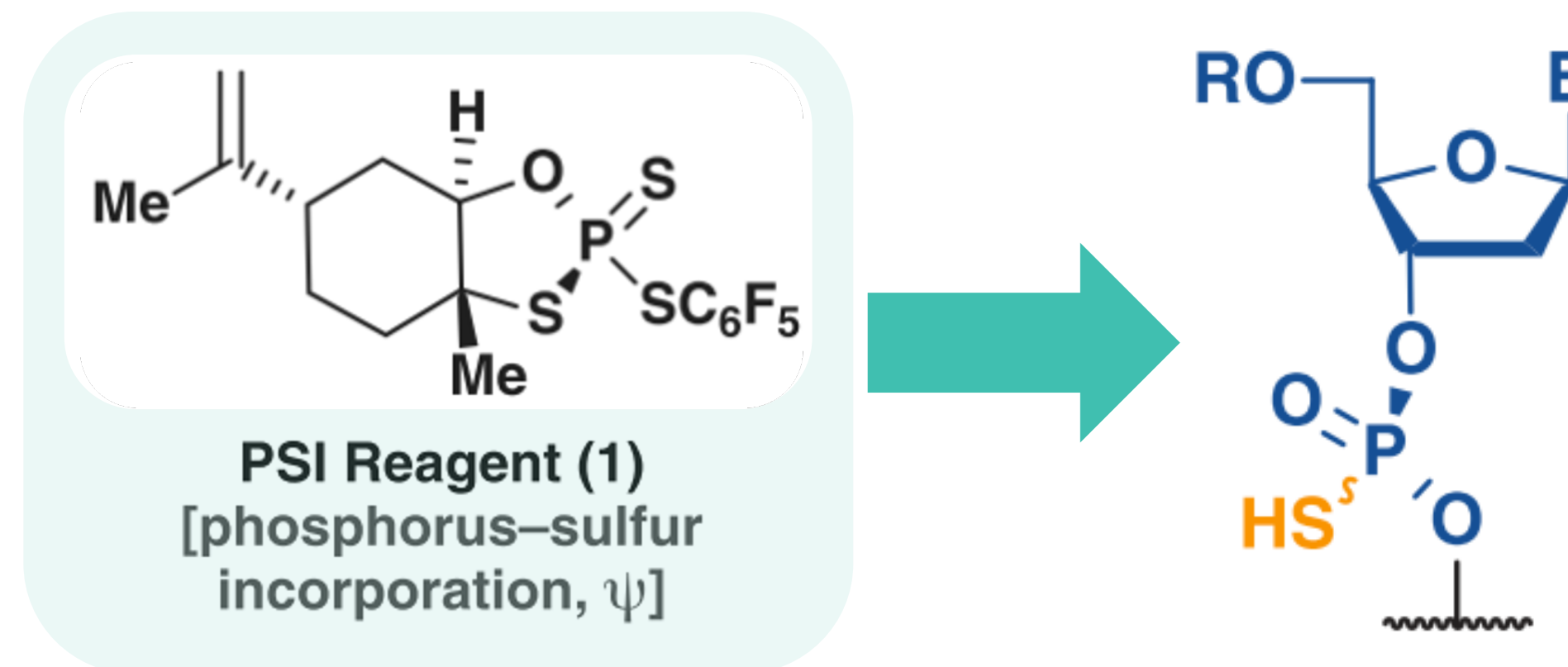


P(V) reagents for stereodivergent synthesis of phosphothioate



Literature Seminar M2 Fujiyoshi 2021/7/29

Contents

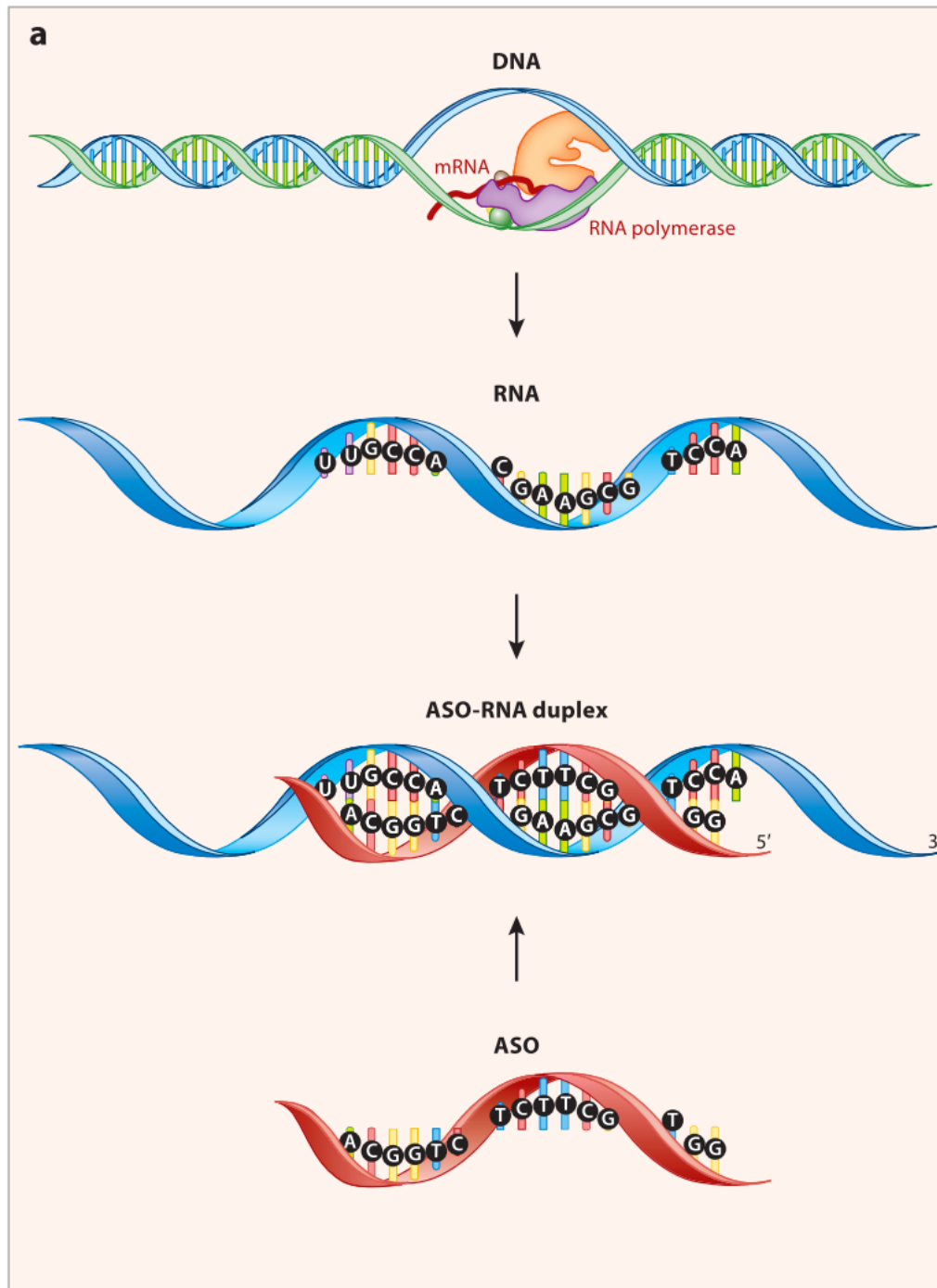
- Introduction of antisense oligonucleotide
- Reagents for chiral phosphorothioate synthesis: ψ reagent
- The principle of ψ reagent's reactivity
 - Stereoselectivity
 - Chemoselectivity
 - High reactivity
- Summary

Contents

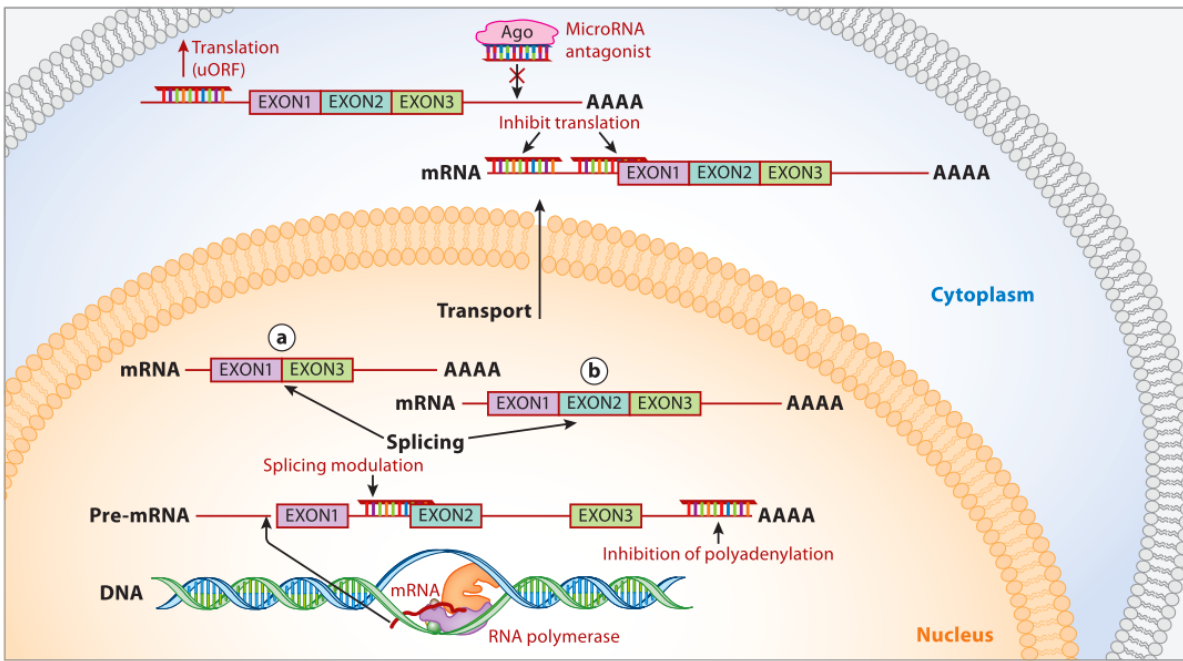
- Introduction of antisense oligonucleotide
- Reagents for chiral phosphorothioate synthesis: ψ reagent
- The principle of ψ reagent's reactivity
 - Stereoselectivity
 - Chemoselectivity
 - High reactivity
- Summary

Antisense Oligonucleotide (ASO)

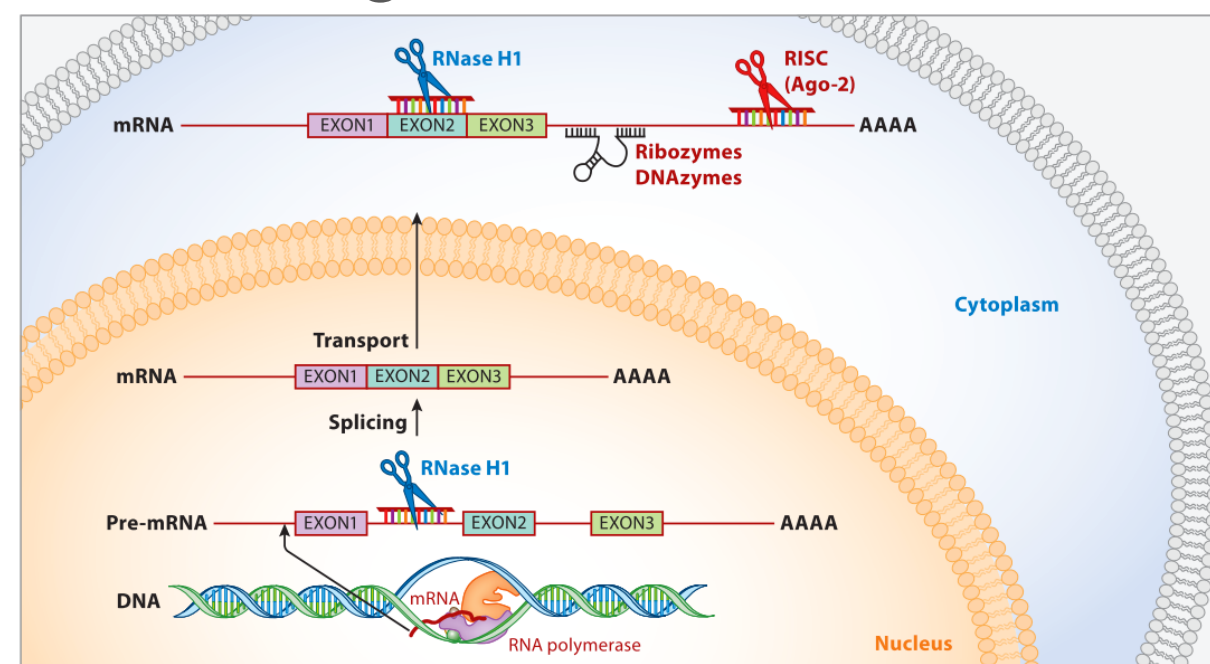
ASO binds to RNA



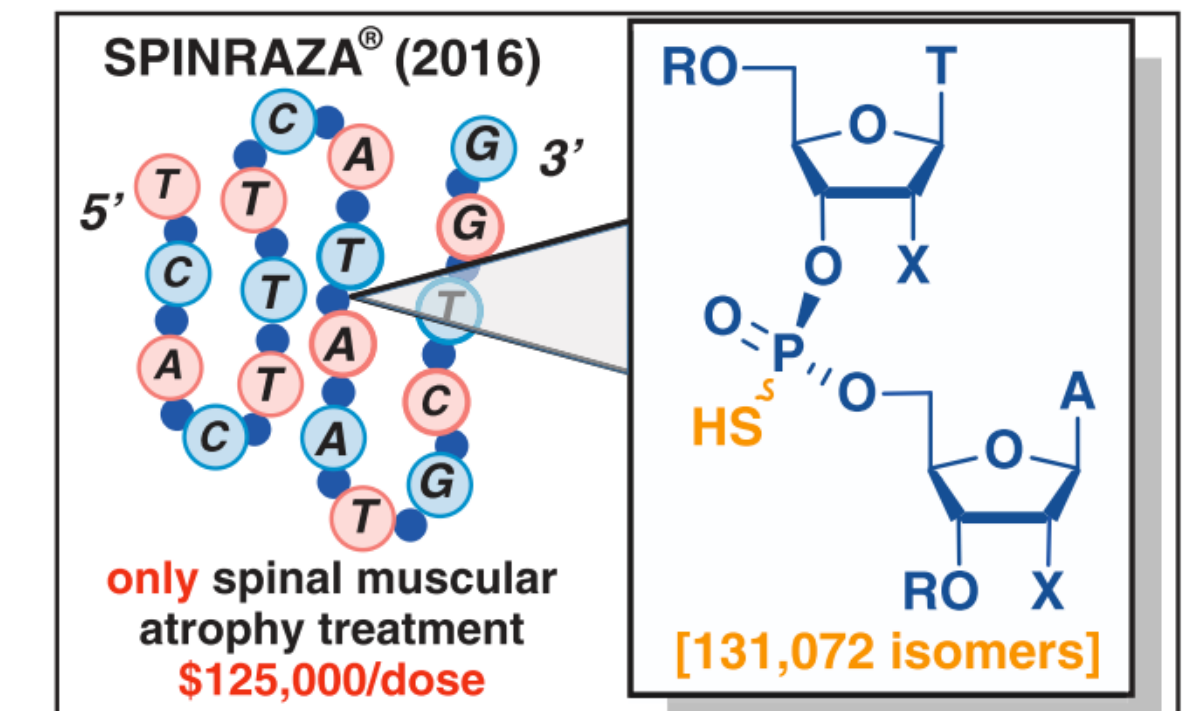
Steric block mechanism



RNA degradation mechanism

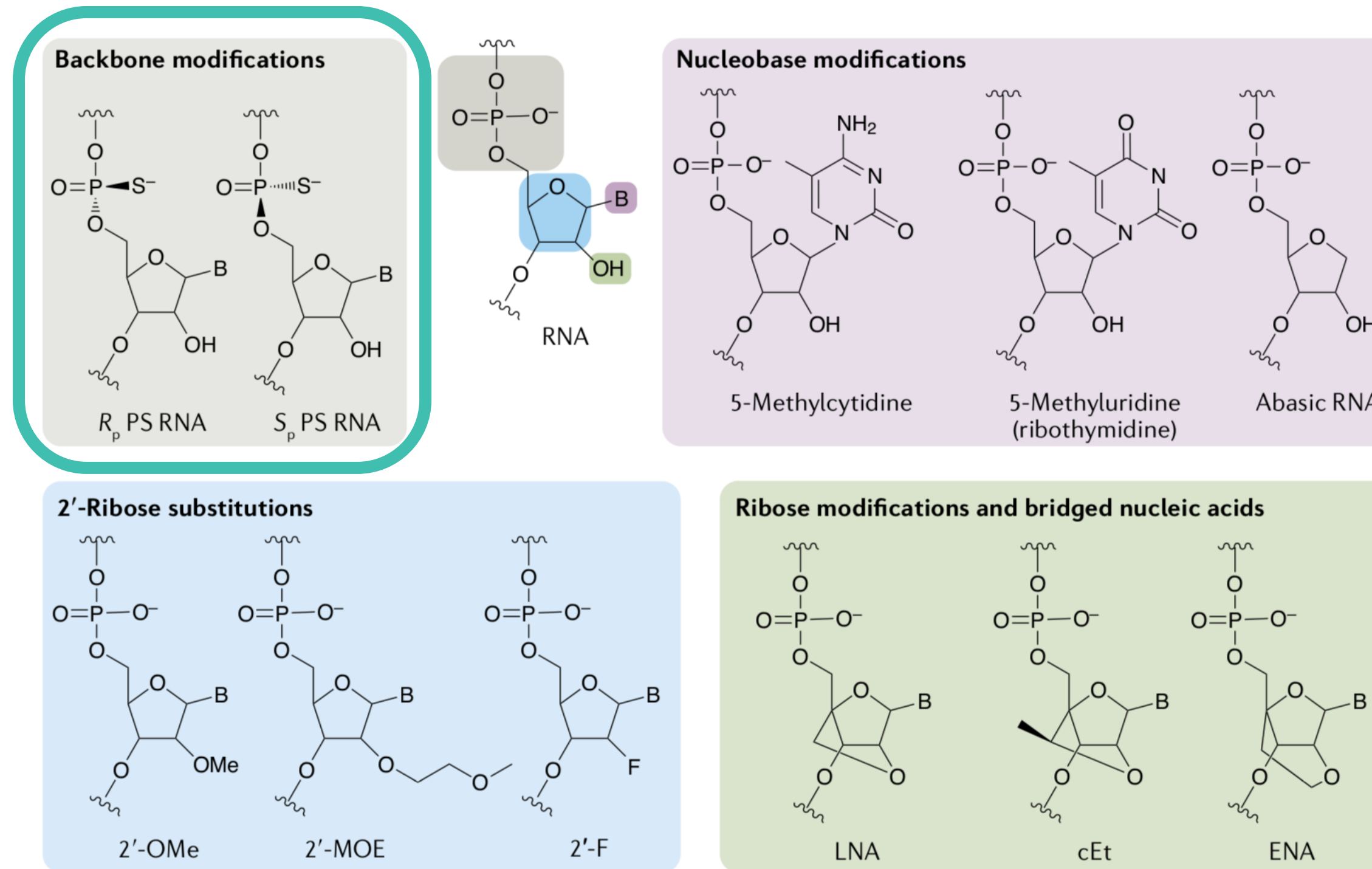


One of the FDA approved ASOs

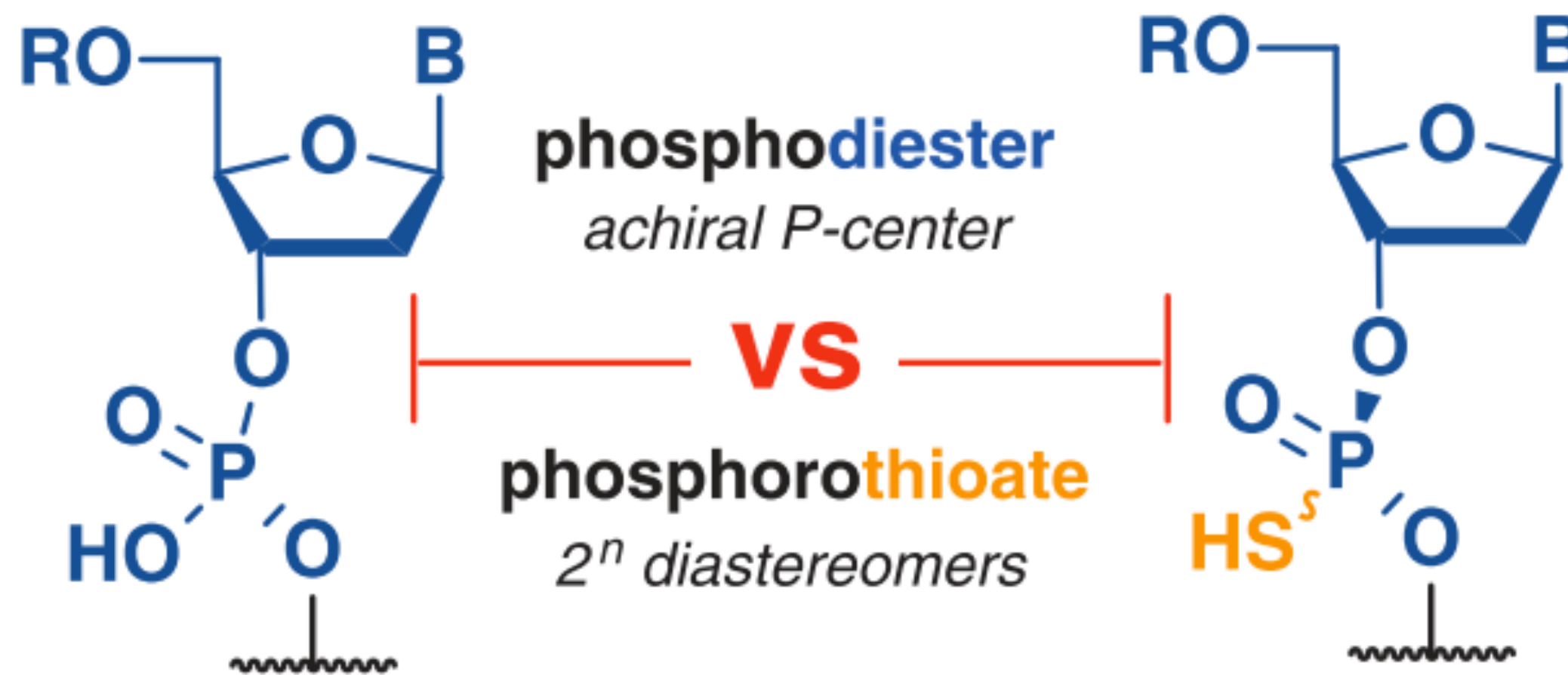


Knouse, K. W.; Baran, P.; et al. *Science*, 2018, 361, 1234

Common chemical modifications in ASO



Why Sulfur? The Thio effect



- **improved cellular uptake**
- **increased stability toward nucleases**

Knouse, K. W.; Baran, P.; *et al. Science*, 2018, 361, 1234

(See latest article for mechanism of cellular uptake)

Laurent, Q.; *et al. Angew. Chem. Int. Ed.* 2021, 60, 1)

The stereochemistry at phosphorus

The stereochemistry of phosphorothioate affect

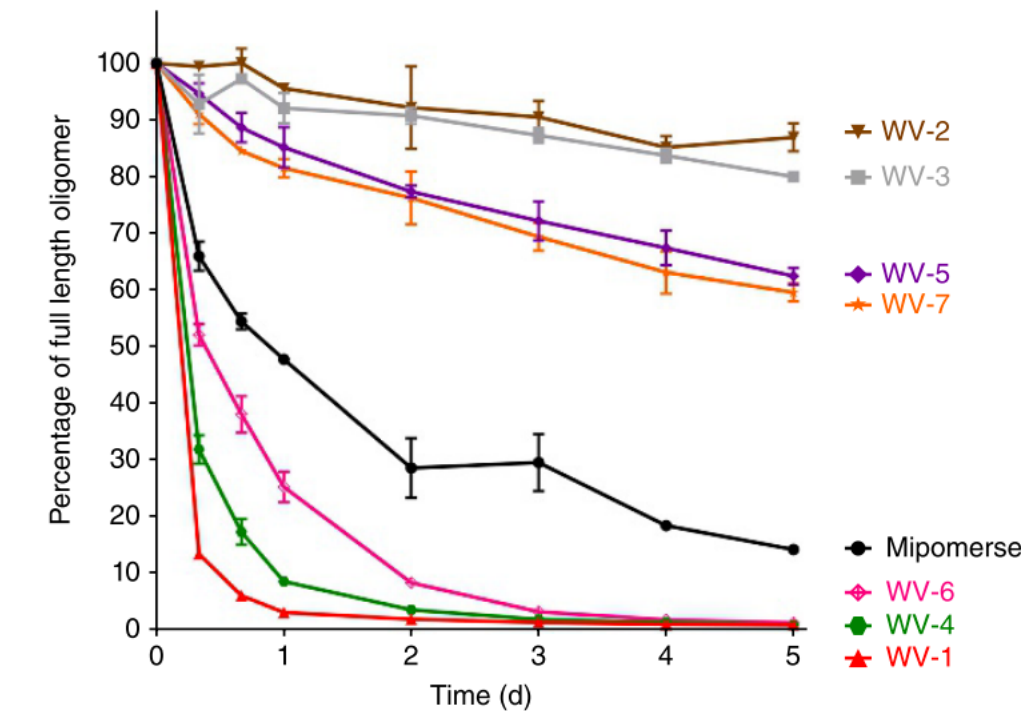
- the stability against nucleases
- the efficiency of degradation of the targeted RNA.

Mipomersen and stereochemically pure counterparts

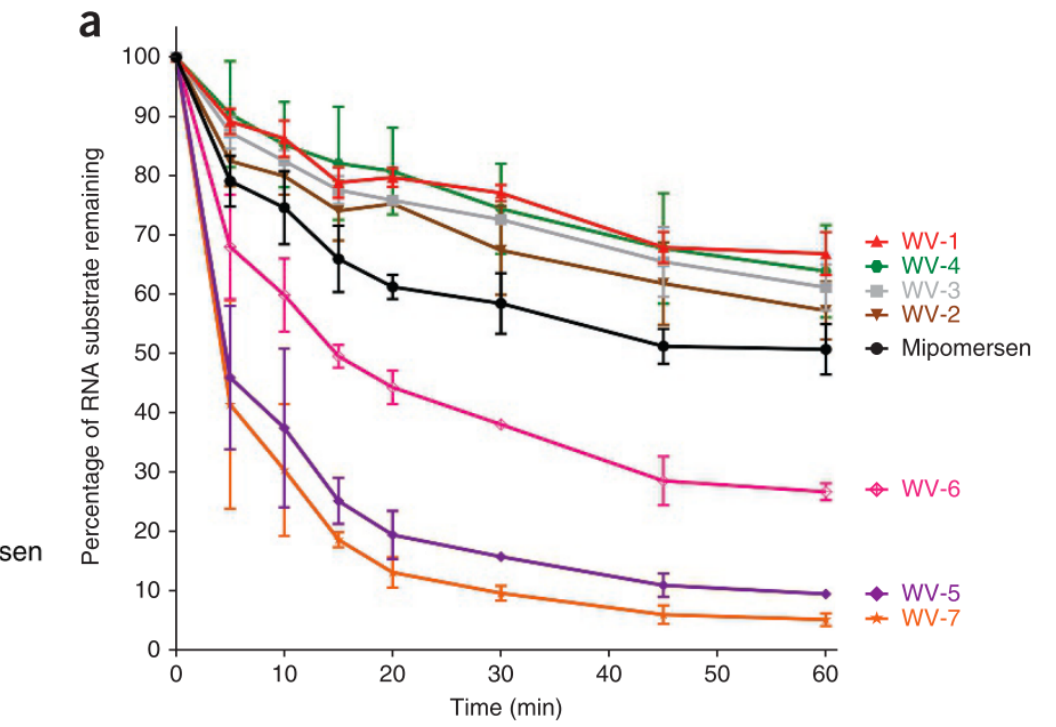
ASO	Sequence	Number of stereoisomer	Tm (°C)	V0 (μM/min)
Mipomersen		524,288	80.2	0.05
WV-1		1	84.7	---
WV-2		1	74.7	---
WV-3		1	78.8	---
WV-4		1	80.0	---
WV-5		1	81.6	0.13
WV-6		1	78.3	---
WV-7		1	68.2	---

◆ Stereorandom ▲ Rp ▽ Sp
○ DNA ◇ 5-Methyl DNA ● 2'-Methoxyethyl (MOE) ■ 5-Methyl 2'-Methoxyethyl (MOE)

Stability in rat liver homogenate

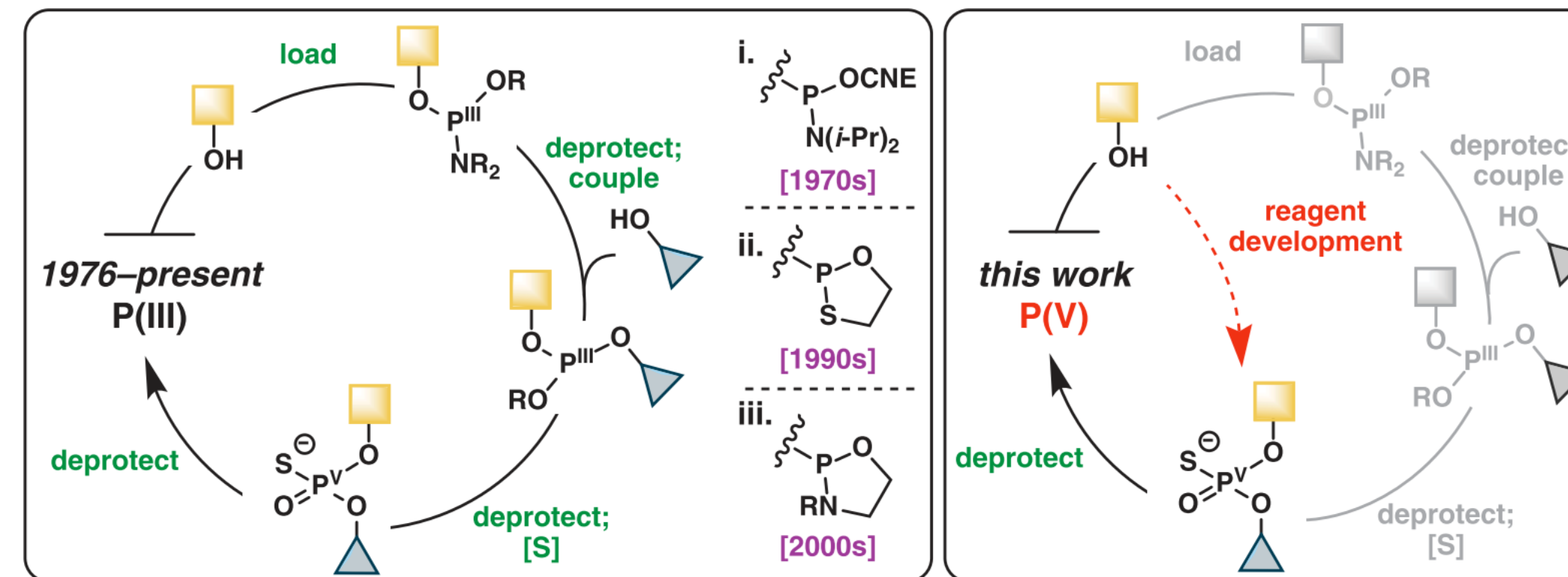


Activity of RNase HC on ASO–RNA heteroduplexes

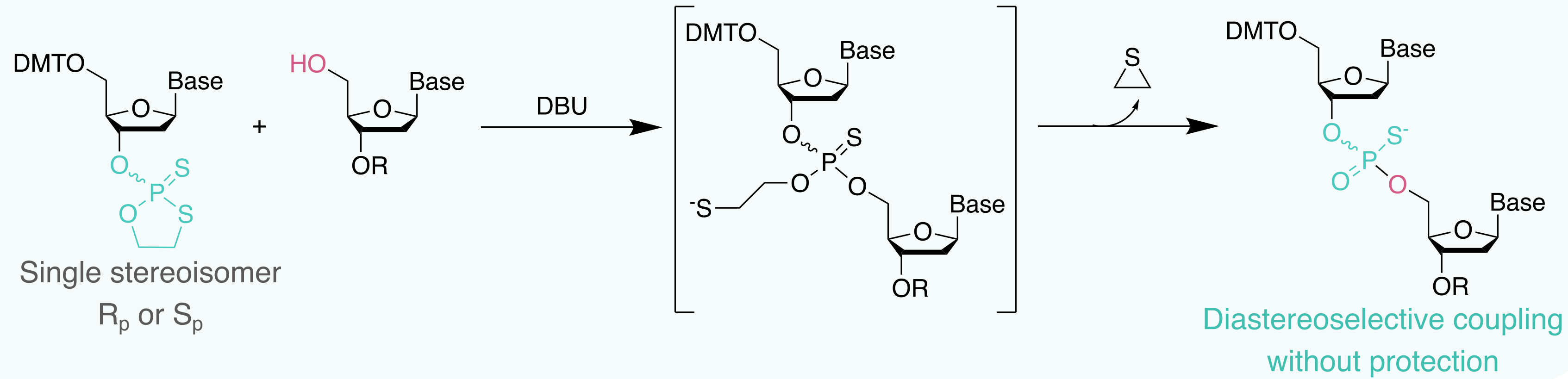


What are problems of current methods for construction of PS linkage?

- Stepwise-synthesis using P(III) chemistry is **operationally cumbersome**.
- P(III) reagent is **air and moisture sensitive**.
- The **stereochemistry** at phosphorus is often disregarded in scalable preparation.



5'-O-DMT-nucleoside 3'-O-(2-thio-1,3,2-oxathiaphospholane)

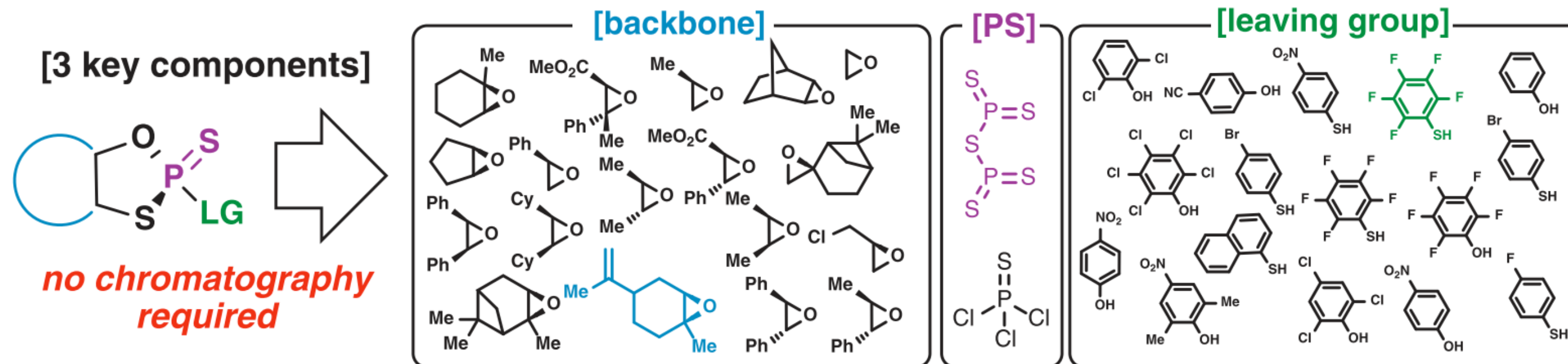


Problems

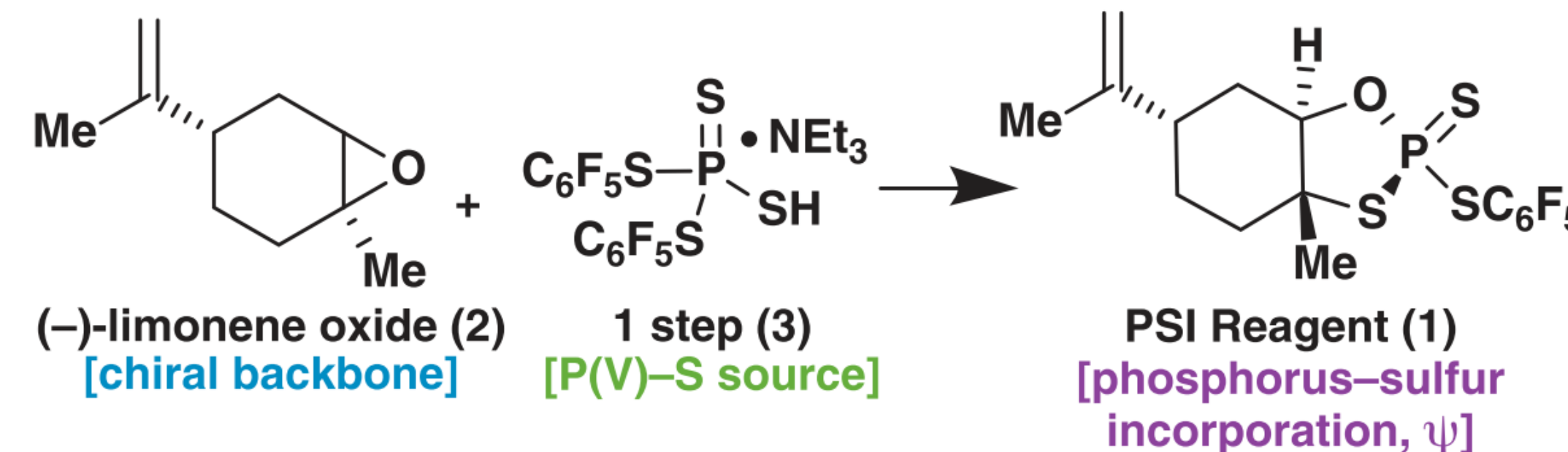
- 3(4) step synthesis of nucleotide loaded reagent **via phosphoramidite P(III)** (See appendix)
- **Separation of the diastereomers of reagents**
- **Scale limited**

Phosphorus–Sulfur Incorporated (PSI, ψ) reagent

C Bypassing P(III): The Quest to Develop an Ideal P(V) Reagent



D PSI Reagent: A Simple, Redox-Economic Alternative

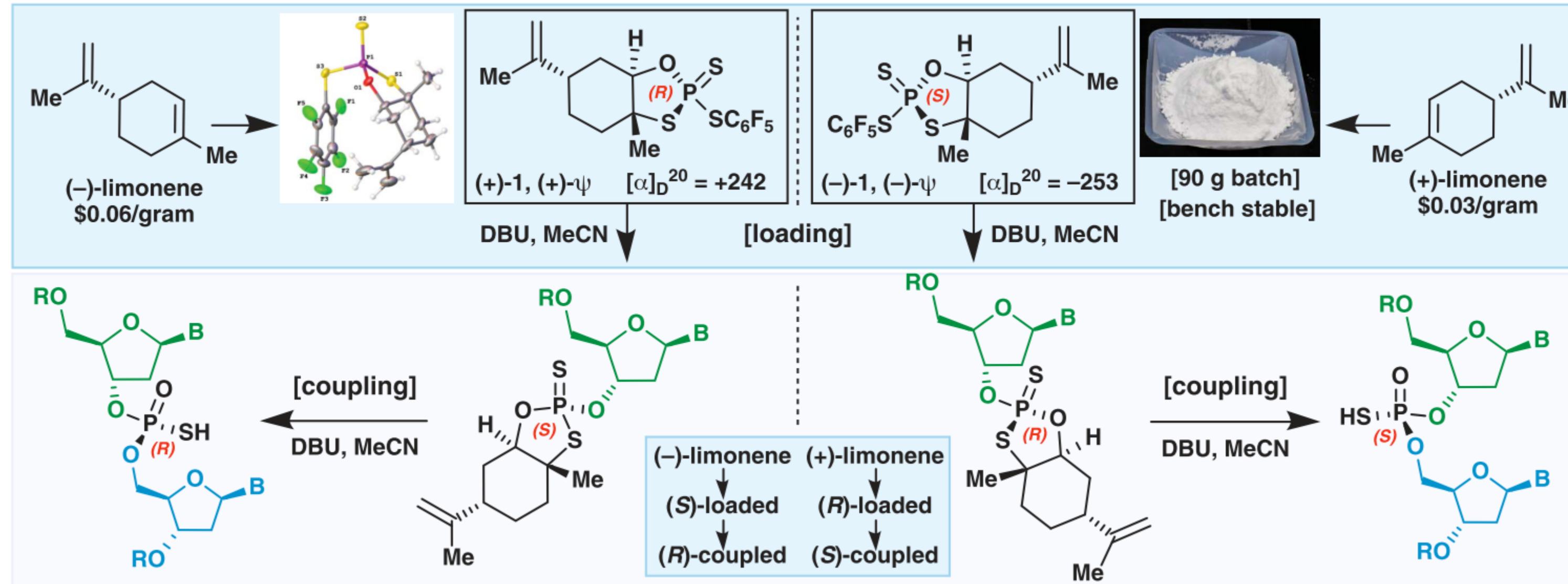


Contents

- Introduction of antisense oligonucleotide
- Reagents for chiral phosphorothioate synthesis: ψ reagent
- The principle of ψ reagent's reactivity
 - Stereoselectivity
 - Chemoselectivity
 - High reactivity
- Summary

Synthesis and Stereochemistry of ψ reagents

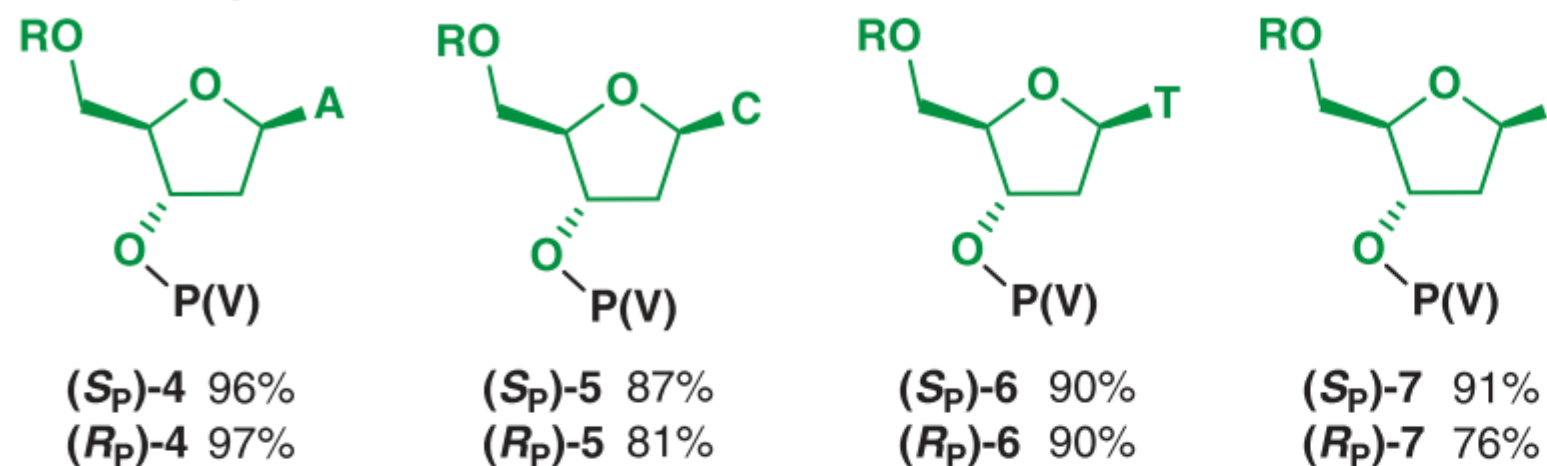
Loading condition: alcohol 1.0 eq., ψ 1.3 eq., DBU 1.3 eq., MeCN, 25 °C, 30 min



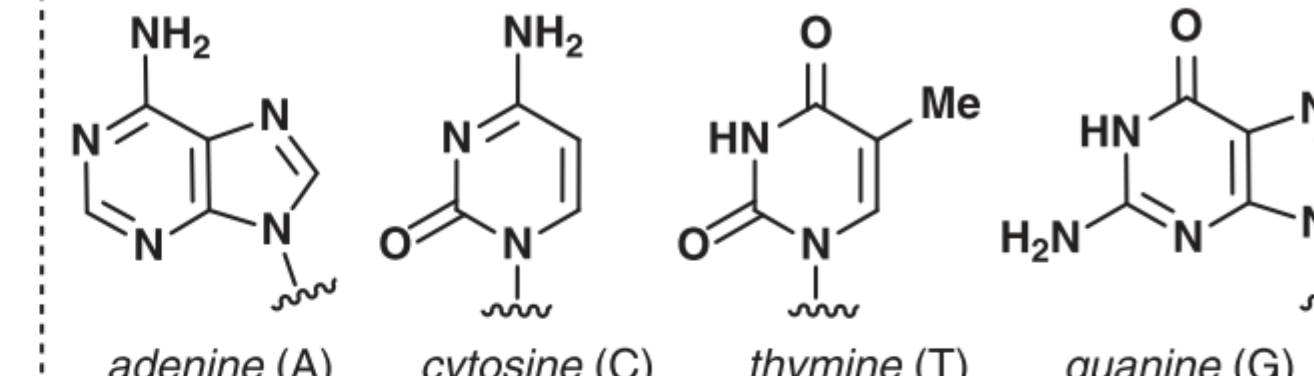
Coupling condition: alcohol 2.0 eq., Nucleoside P(V) 1.0 eq., DBU 3.0 eq., MeCN, 25 °C, 30 min

Loading and Coupling of Nucleosides with ψ reagents

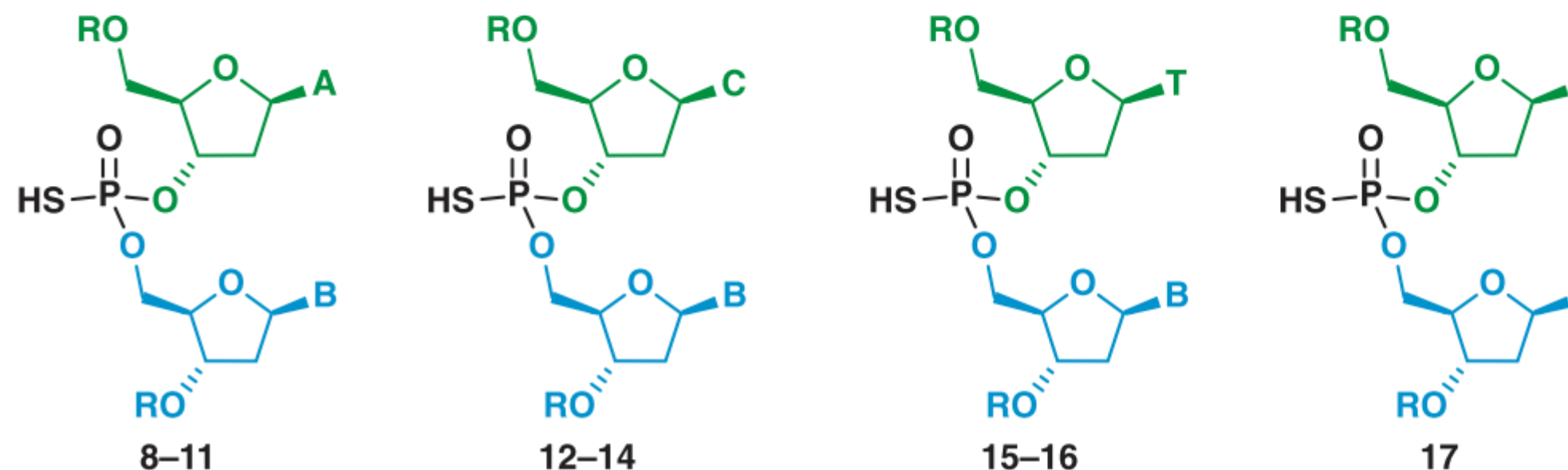
B Loaded ψ Nucleosides



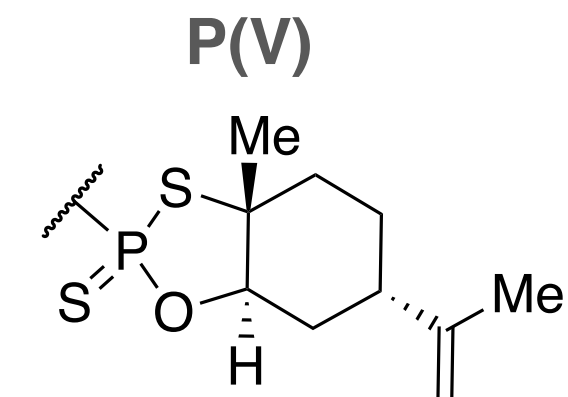
Unprotected Nucleobases:



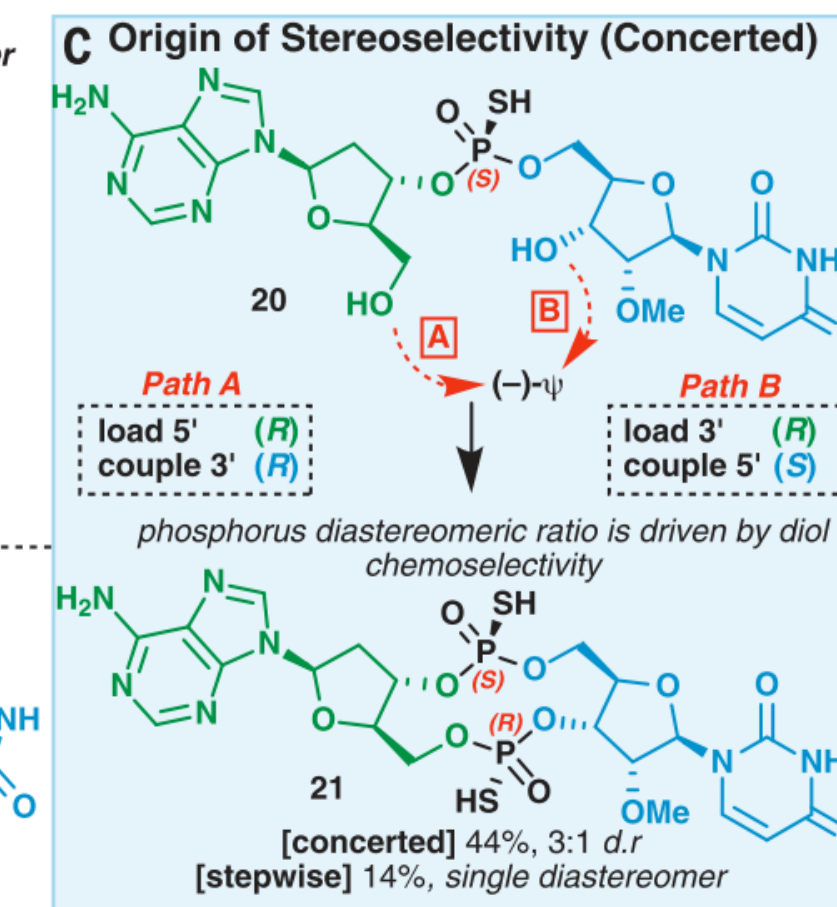
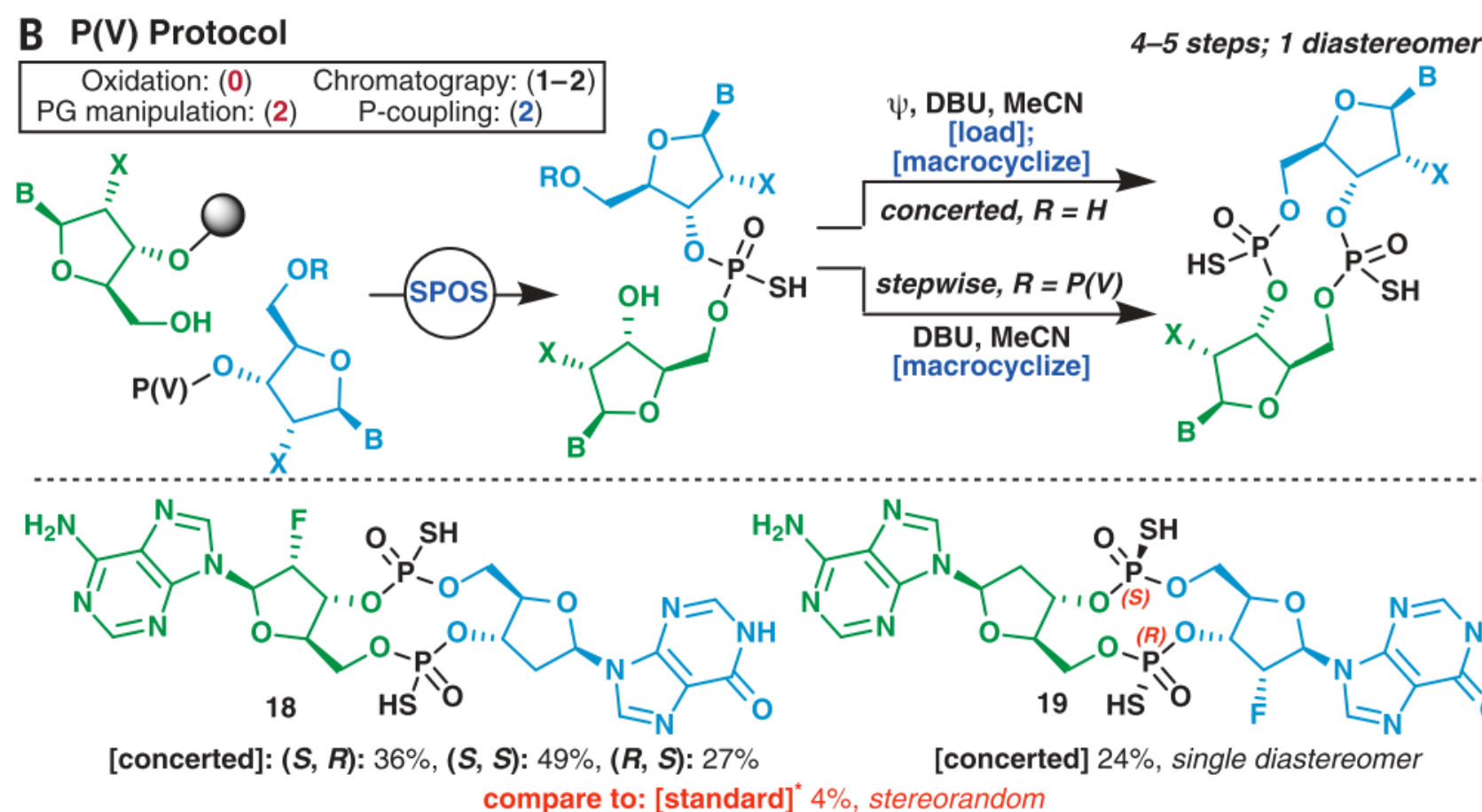
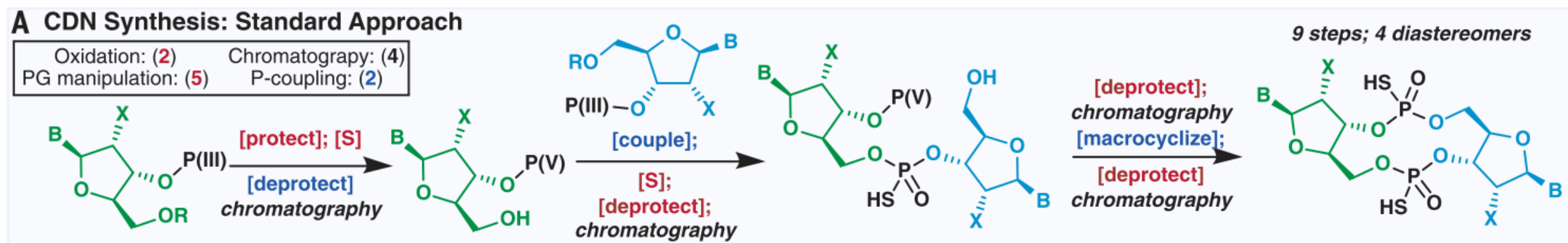
C Coupled ψ Nucleosides



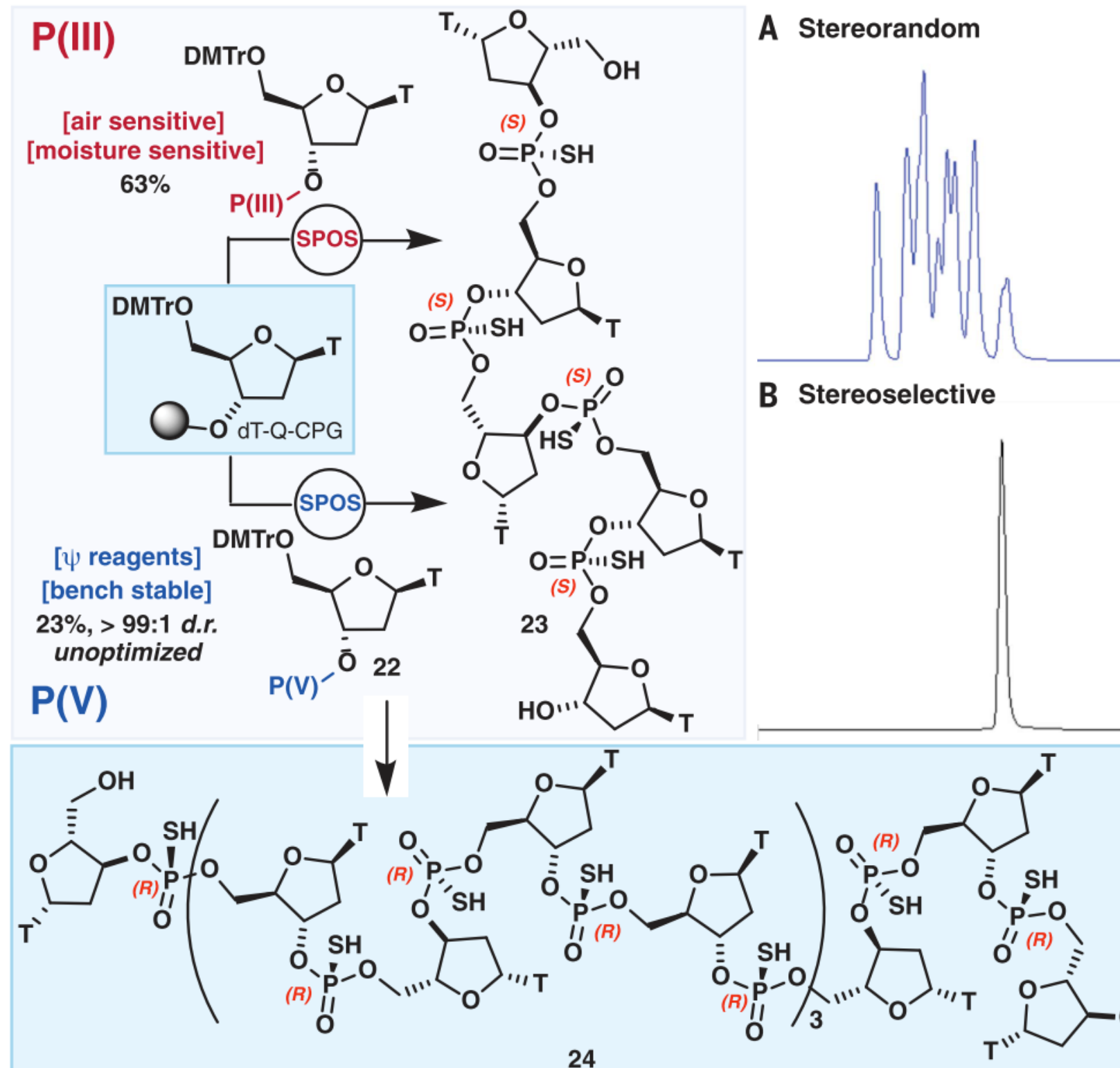
dinucleotide	yield (d.r.)
8, dA-dA (<i>R_P</i>)	65% (>99:1)
9, dA-dC (<i>S_P</i>)	91% (>99:1)
10, dA-dT (<i>S_P</i>)	61% (>99:1)
11, dA-dG (<i>S_P</i>)	79% (>99:1)
12, dC-dC (<i>R_P</i>)	73% (>99:1)
13, dC-dT (<i>S_P</i>)	76% (>99:1)
14, dC-dG (<i>R_P</i>)	82% (>99:1)
15, dT-dT (<i>S_P</i>)	72% (>99:1)
16, dT-dG (<i>S_P</i>)	67% (>99:1)
17, dG-dG (<i>R_P</i>)	86% (>99:1)



CDN Synthesis: Standard approach vs. ψ reagent platform



Automated synthesis of PS oligonucleotides

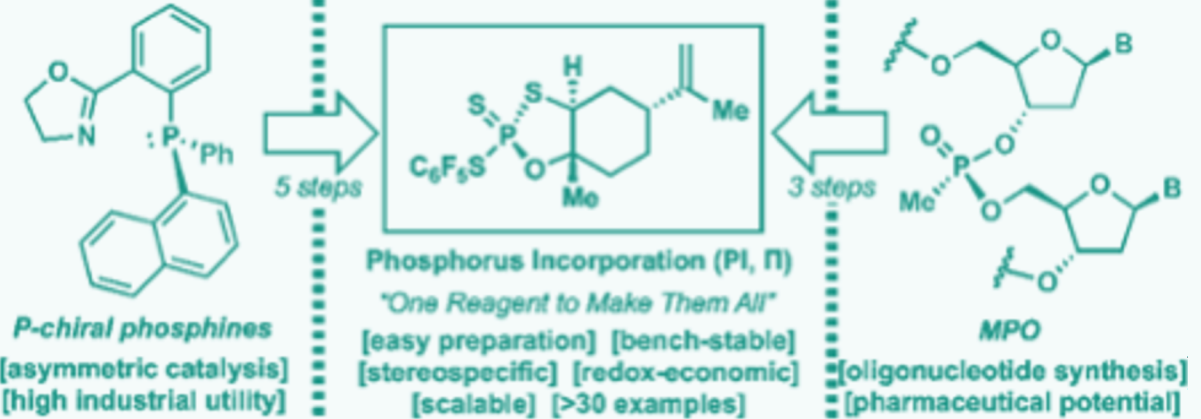


- ψ reagent can be utilized in stereoselective SPOS.

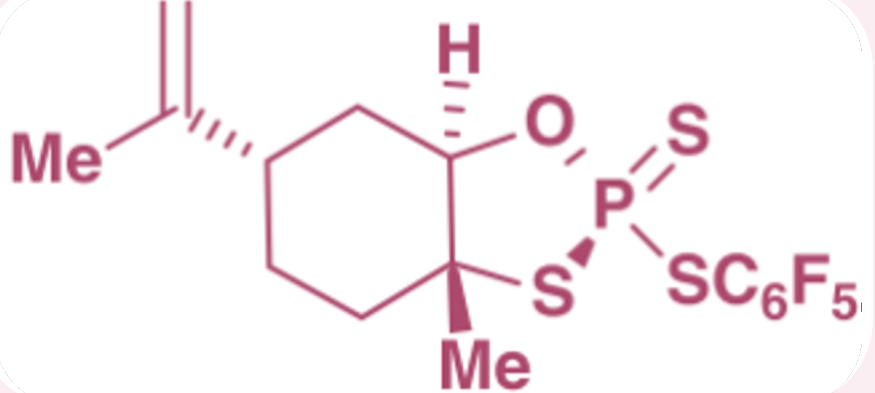
Fig. 4. Automated synthesis of PS oligonucleotides. (A) Crude HPLC trace of pentamer **23** (16 diastereoisomers) synthesized under standard P(III) automated conditions. (B) Crude HPLC trace of pentamer **23** (1 diastereoisomer) synthesized under unoptimized ψ automated conditions. DMTr, dimethoxytrityl.

Other applications of ψ reagents

Enantiodivergent formation of C–P bond



Xu, D.; Baran, P.; et al. *J. Am. Chem. Soc.* 2020, 142, 5785

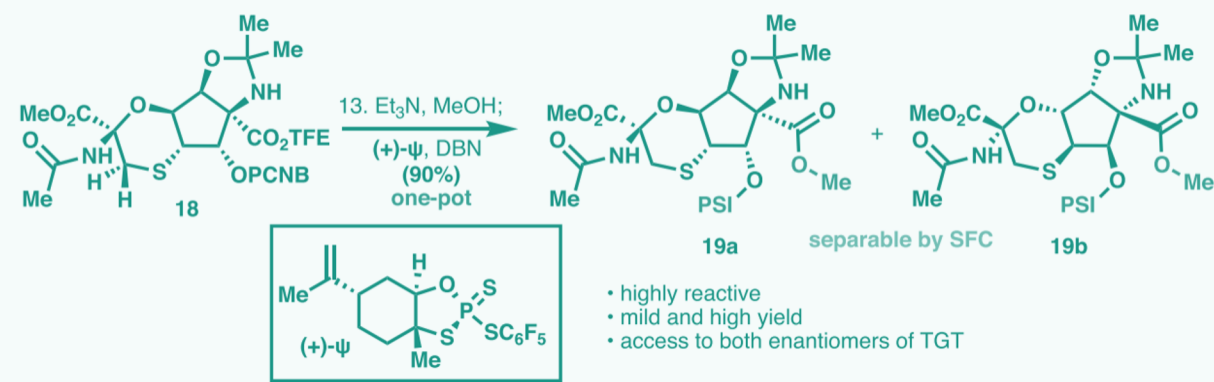


Native DNA manipulation



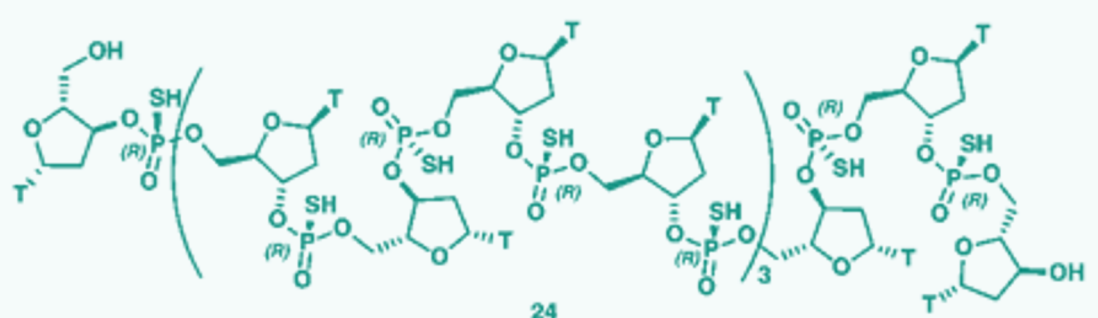
Flood, D. T.; Baran, P.; et al., *ACS Cent. Sci.* 2020, 6, 1789

Total Synthesis of Tagetitoxin



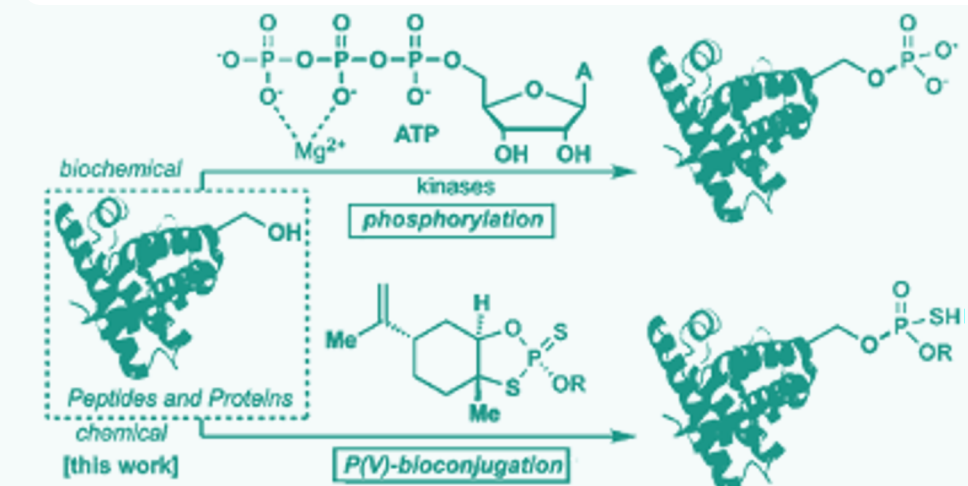
He, C.; Baran, P.; et al. *J. Am. Chem. Soc.* 2020, 142, 13683

Oligonucleotide synthesis



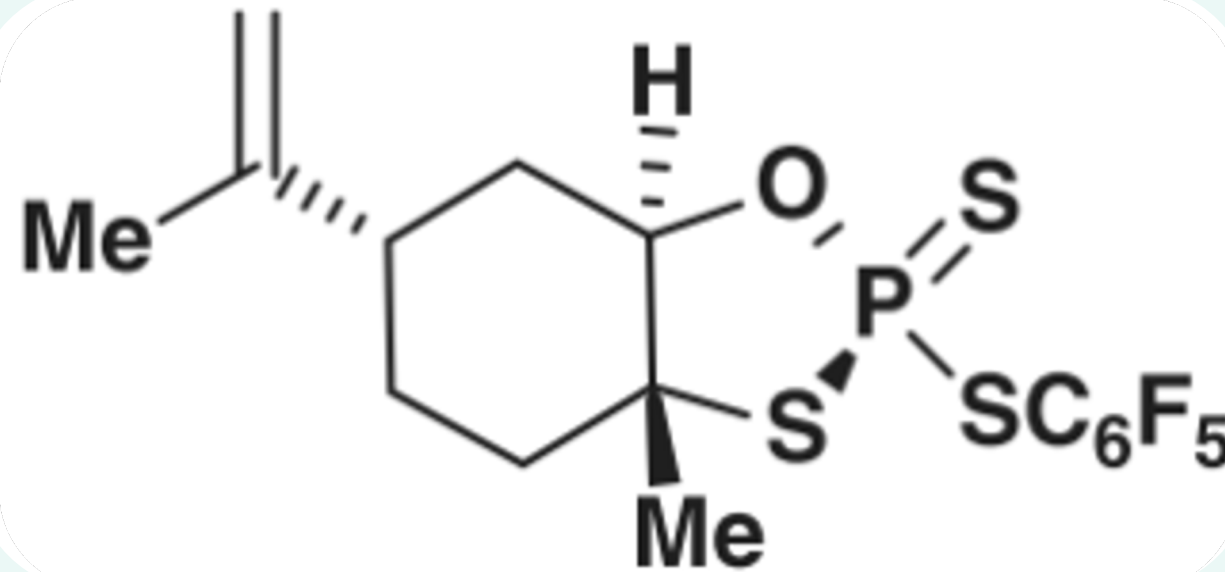
Knouse, K. W.; Baran, P.; et al. *Science*, 2018, 361, 1234

Serine selective bioconjugation



Vantourout, J.; Baran, P.; et al. *J. Am. Chem. Soc.* 2020, 142, 17236

Short summary



PSI Reagent (1)
[phosphorus–sulfur
incorporation, ψ]

- Redox-economic
- Bench-stable reagents
- Simplified protocol
- Solid and solution phase
- Rapid and scale amenable
- Highly broad applications other than ASO synthesis

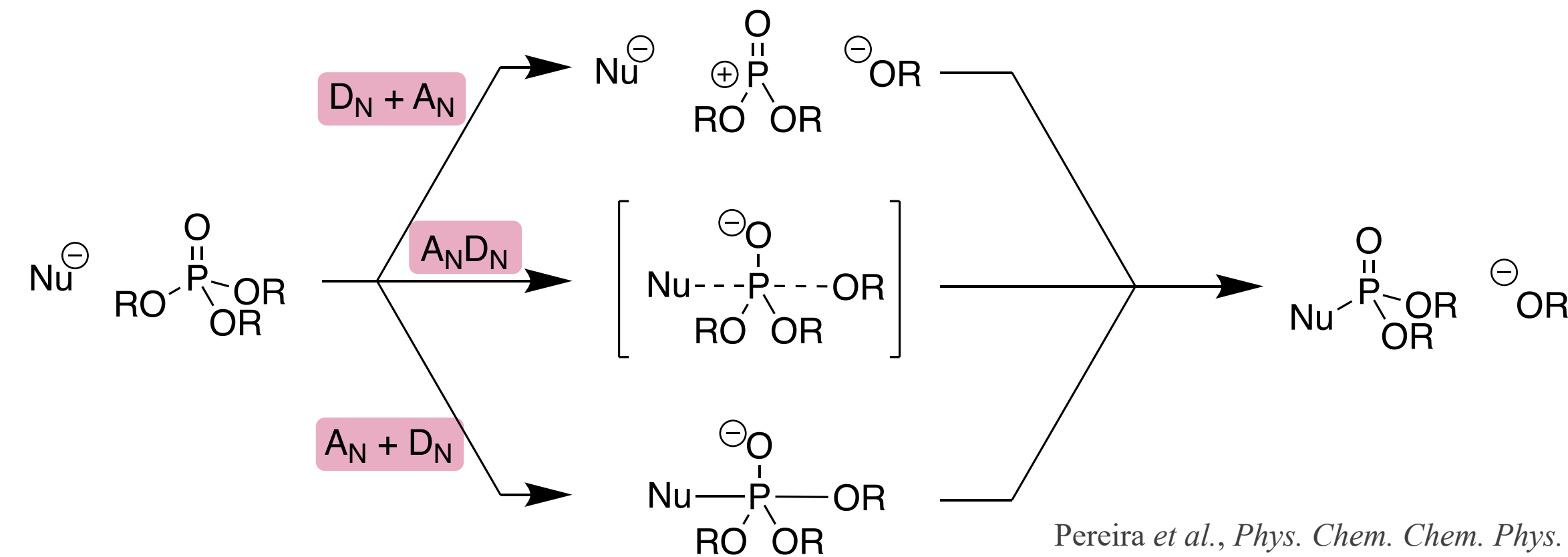
Contents

- Introduction of antisense oligonucleotide
- Reagents for chiral phosphorothioate synthesis: ψ reagent
- The principle of ψ reagent's reactivity
 - Stereoselectivity
 - Chemoselectivity
 - High reactivity
- Summary

The noteworthy points of ψ reagent

- **Stereoselectivity**
 - *d.r.* >99:1 in the synthesis of ASO
- **Chemosselectivity**
 - Serine-selective phosphorylation in the presence of other nucleophiles
- **High reactivity under mild condition**
 - 30 min at r.t. in loading and coupling reaction

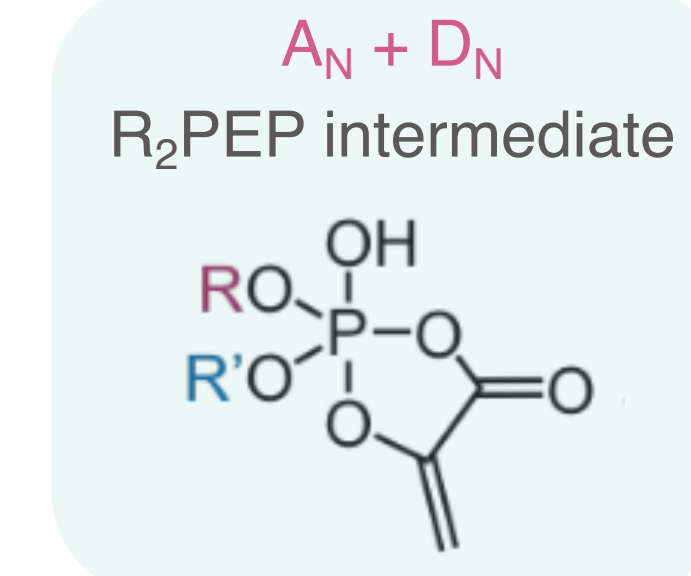
Reaction mechanism of phosphoryl transfer



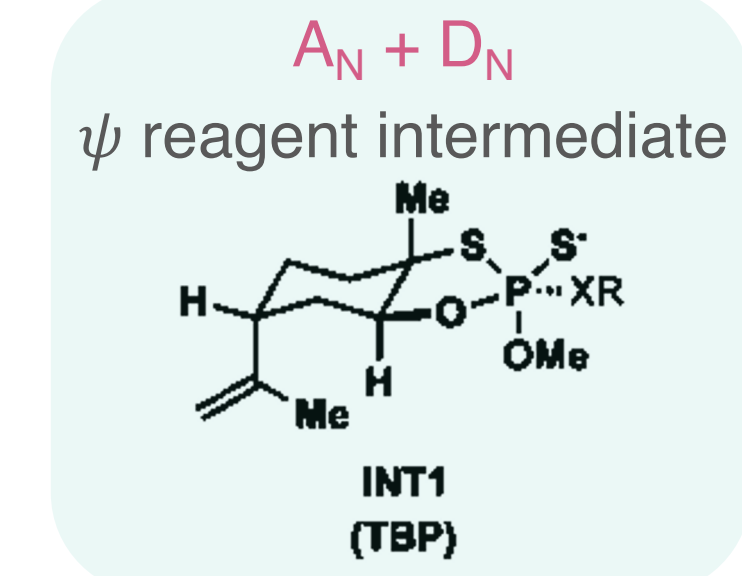
Pereira *et al.*, *Phys. Chem. Chem. Phys.* **2016**, *18*, 18255



Domon, K.; Fujiyoshi, K.; Kanai, M.; *et al.*
ACS Cent. Sci. **2020**, *6*, 283



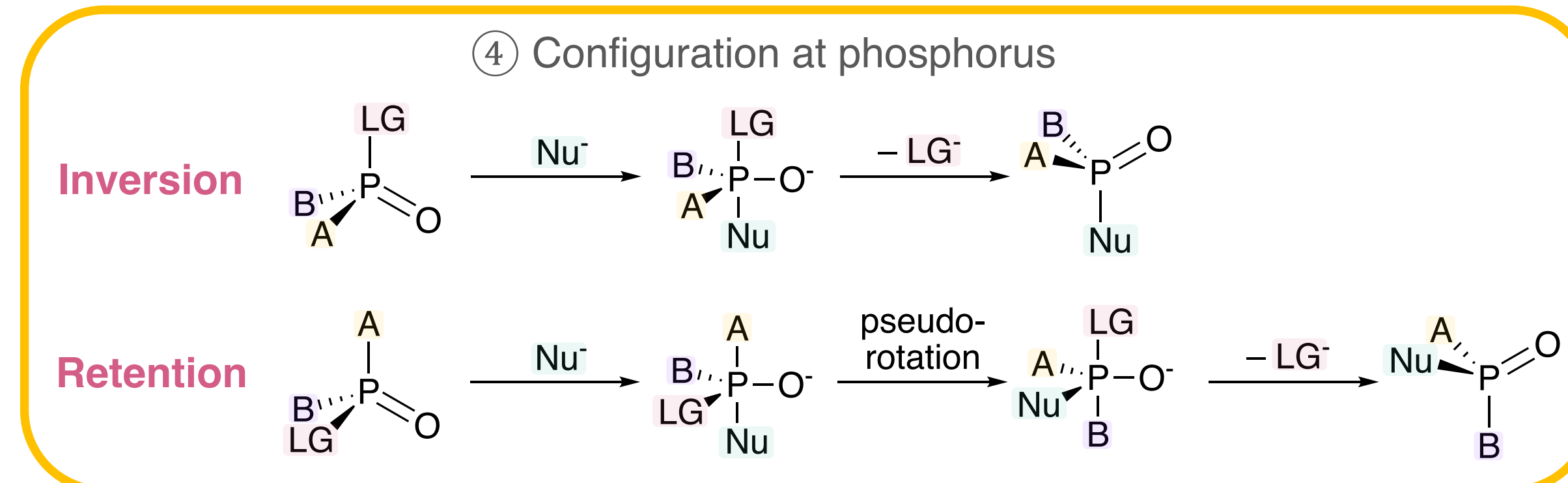
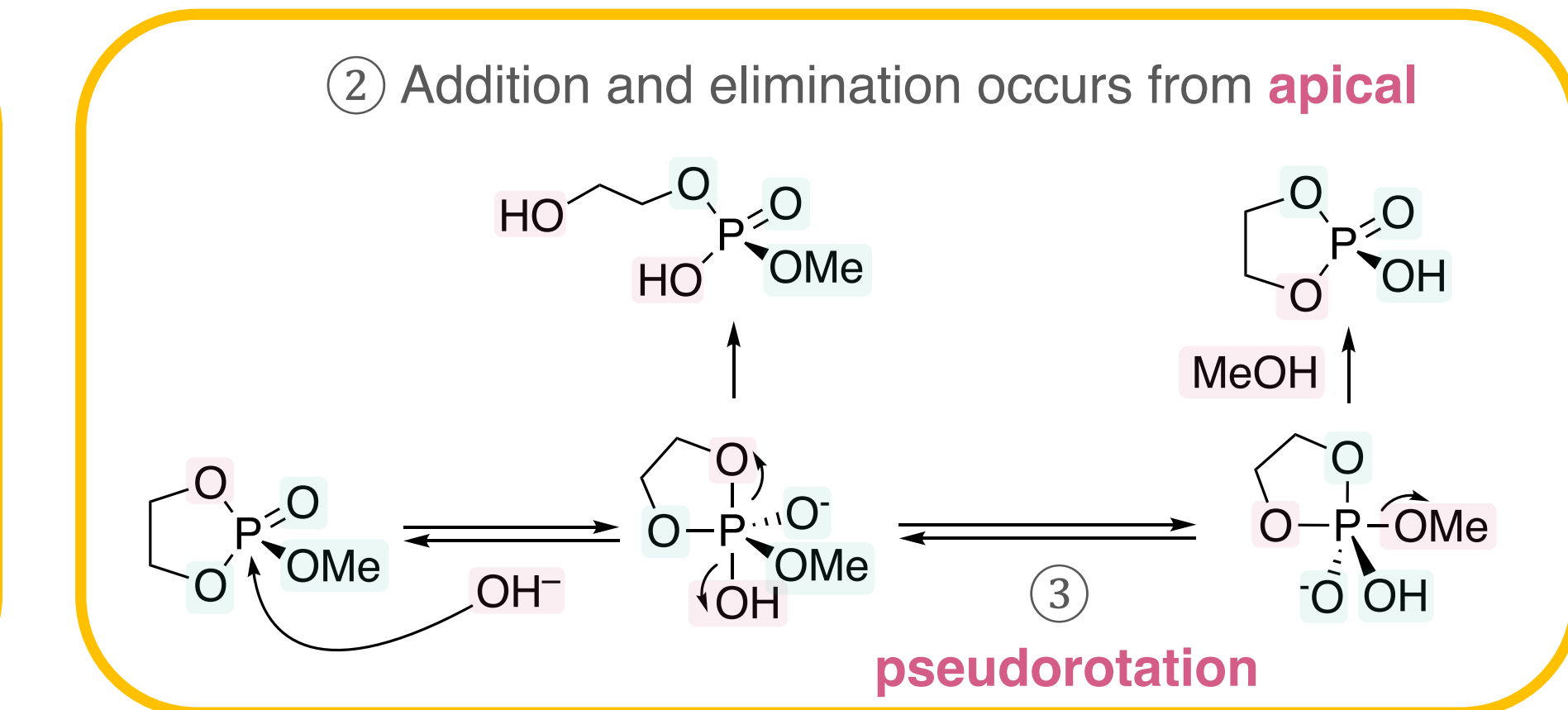
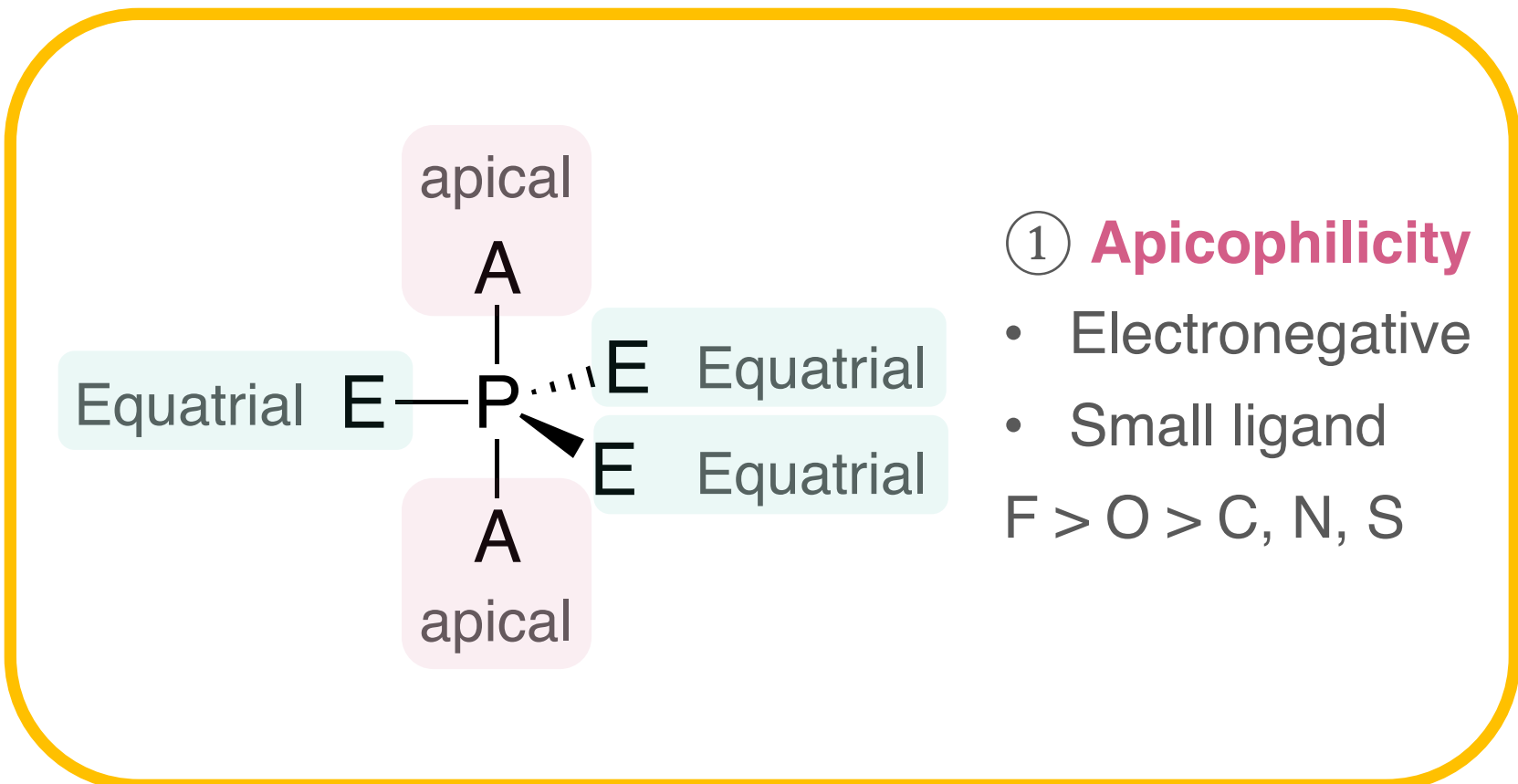
Fujiyoshi, K.; Motomu, K.; *et al.*
Synlett **2021**, *32*, 1135



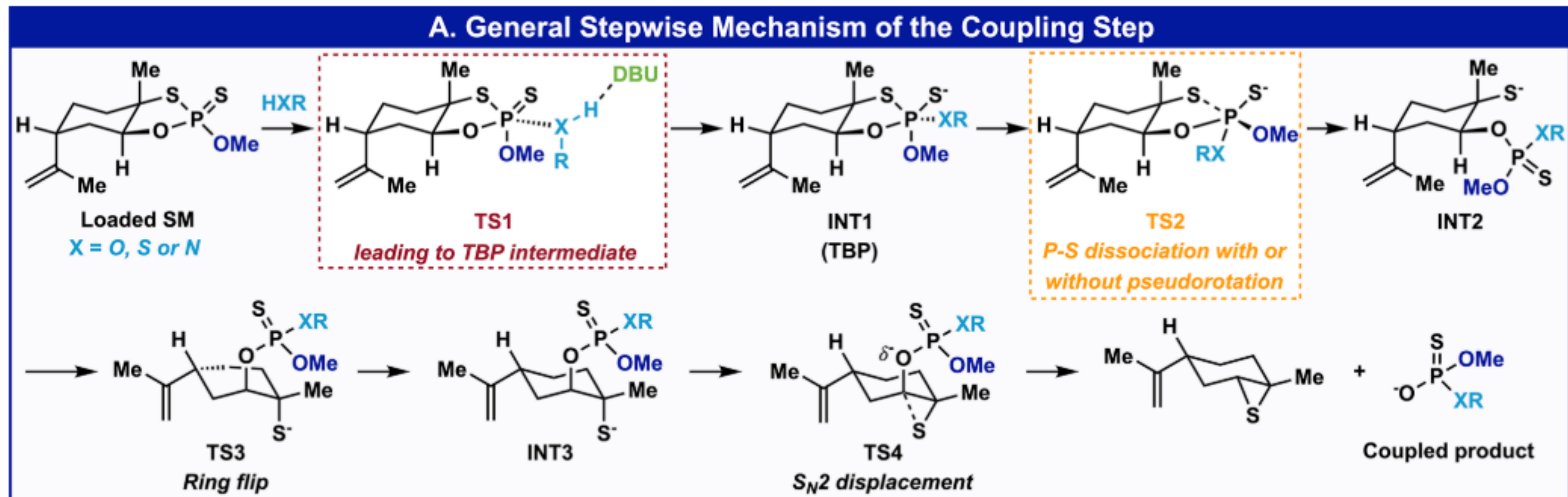
Vantourout, J.; Baran, P.; *et al.*
J. Am. Chem. Soc. **2020**, *142*, 17236

M2 Fujiyoshi

Trigonal-bipyramidal (TBP) phosphorane intermediate



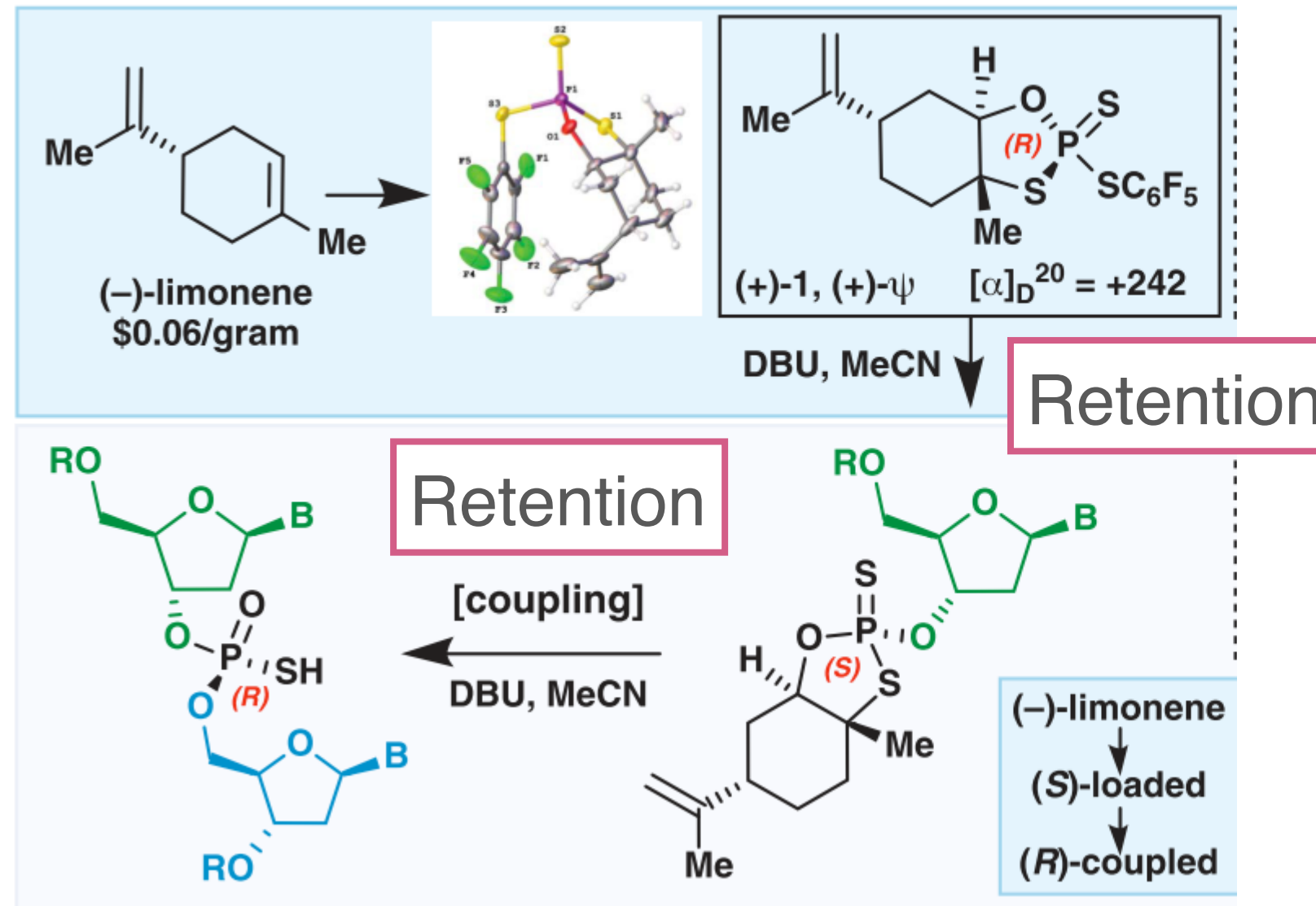
Proposed mechanism



The noteworthy points of ψ reagent

- **Stereoselectivity**
 - *d.r.* >99:1 in the synthesis of ASO
- **Chemosselectivity**
 - Serine-selective phosphorylation in the presence of other nucleophiles
- **High reactivity under mild condition**
 - 30 min at r.t. in loading and coupling reaction

Question: The stereochemistry of ψ reagents

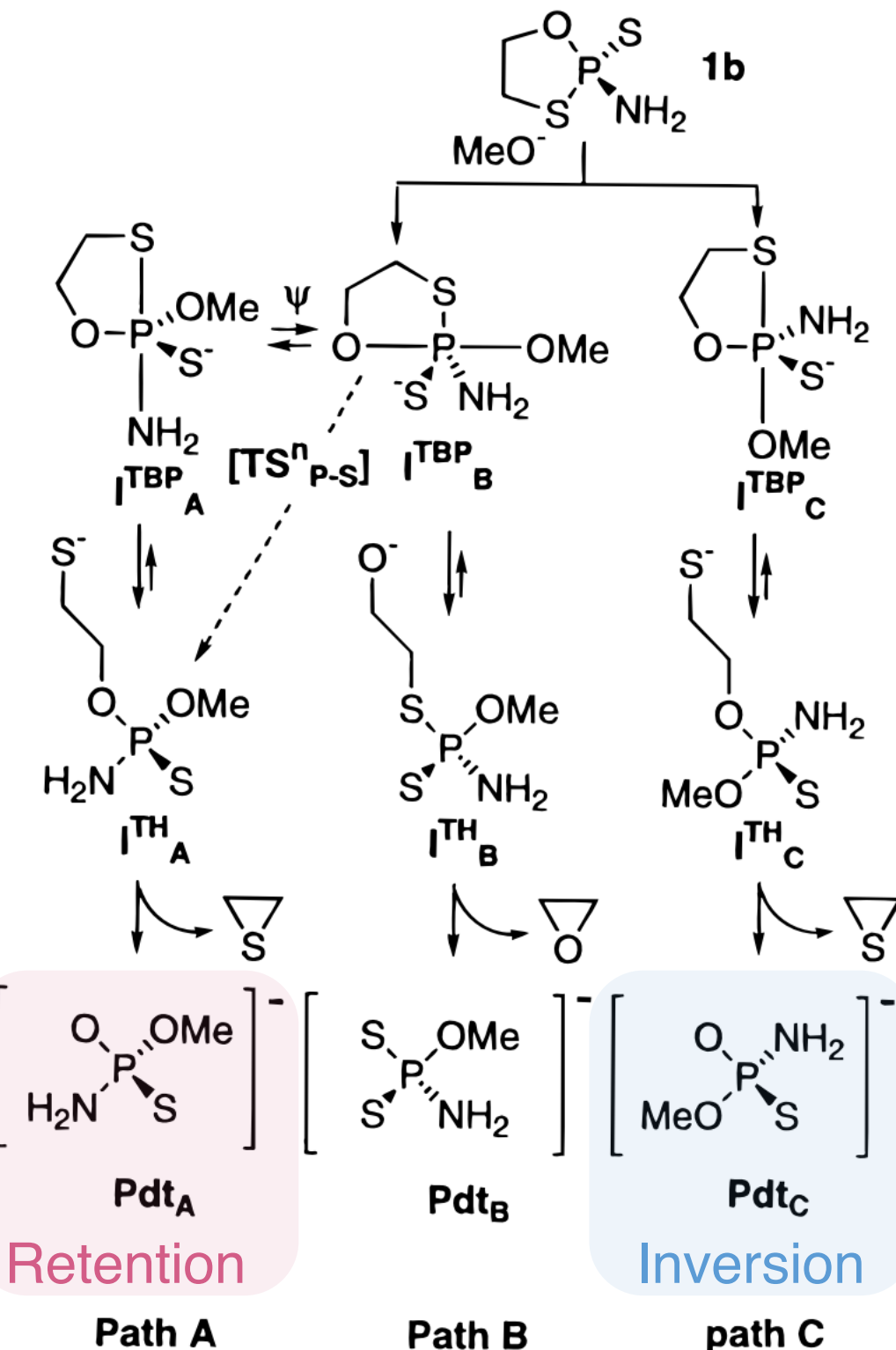


Each loading and coupling step shows a **retention** of configuration at phosphorus.



Why?

Possible pathways for methanolysis of the oxathiaphospholane



The methanolysis of **1b** occurs with a **retention** of configuration at phosphorus.

- To minimize the ring strain, the **five-membered ring** occupies **one apical and one equatorial position** in TBP.
- Anionic S atom derived from P=S is always **equatorial**.

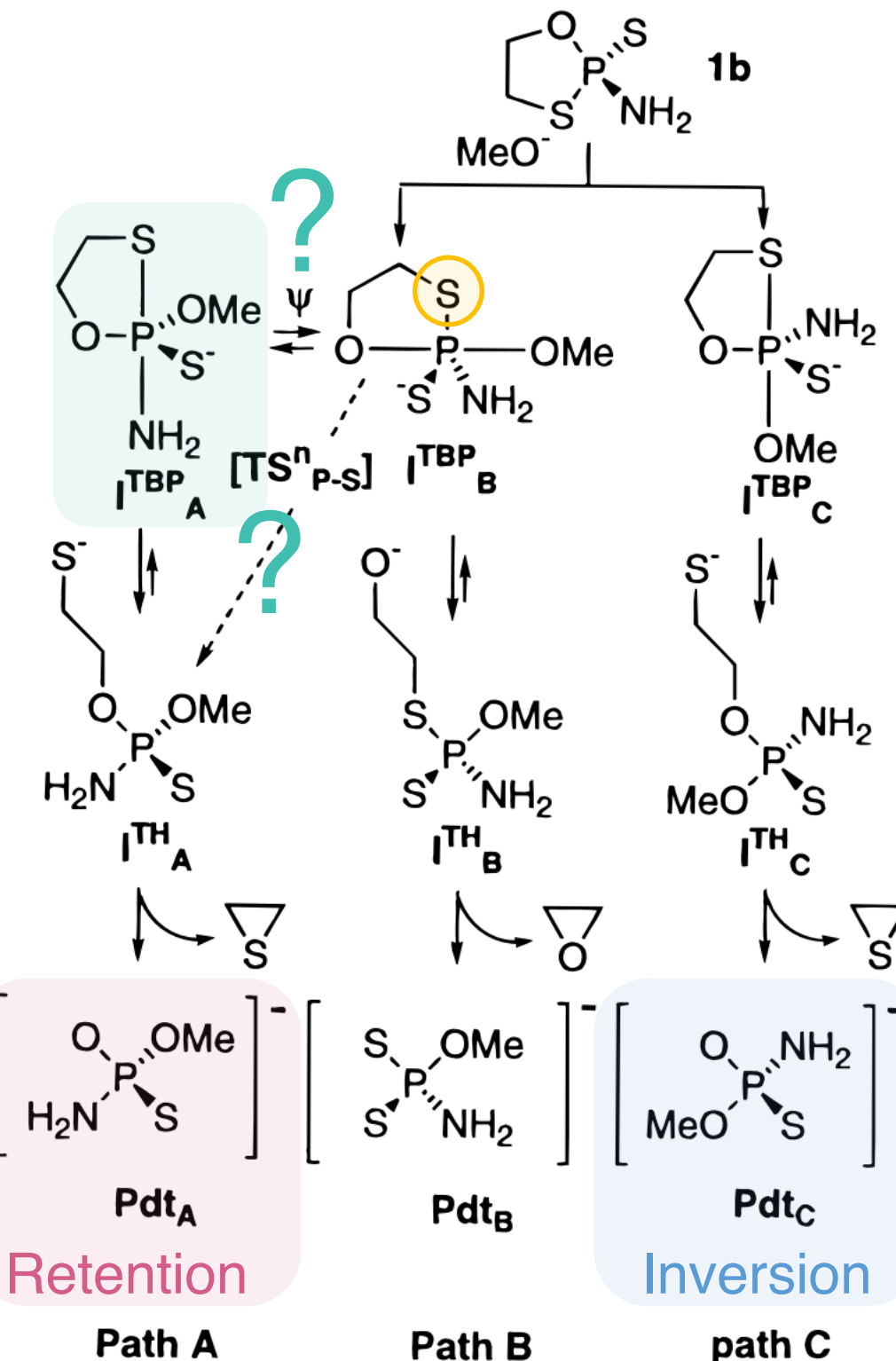
Three pathways A, B and C are possible.

Only path **A** show a **retention** of configuration at phosphorus.

However...

^a ψ indicates a pseudorotation process.

Possible pathways for methanolysis of the oxathiaphospholane



Only path **A** show a **retention** of configuration at phosphorus.

However...

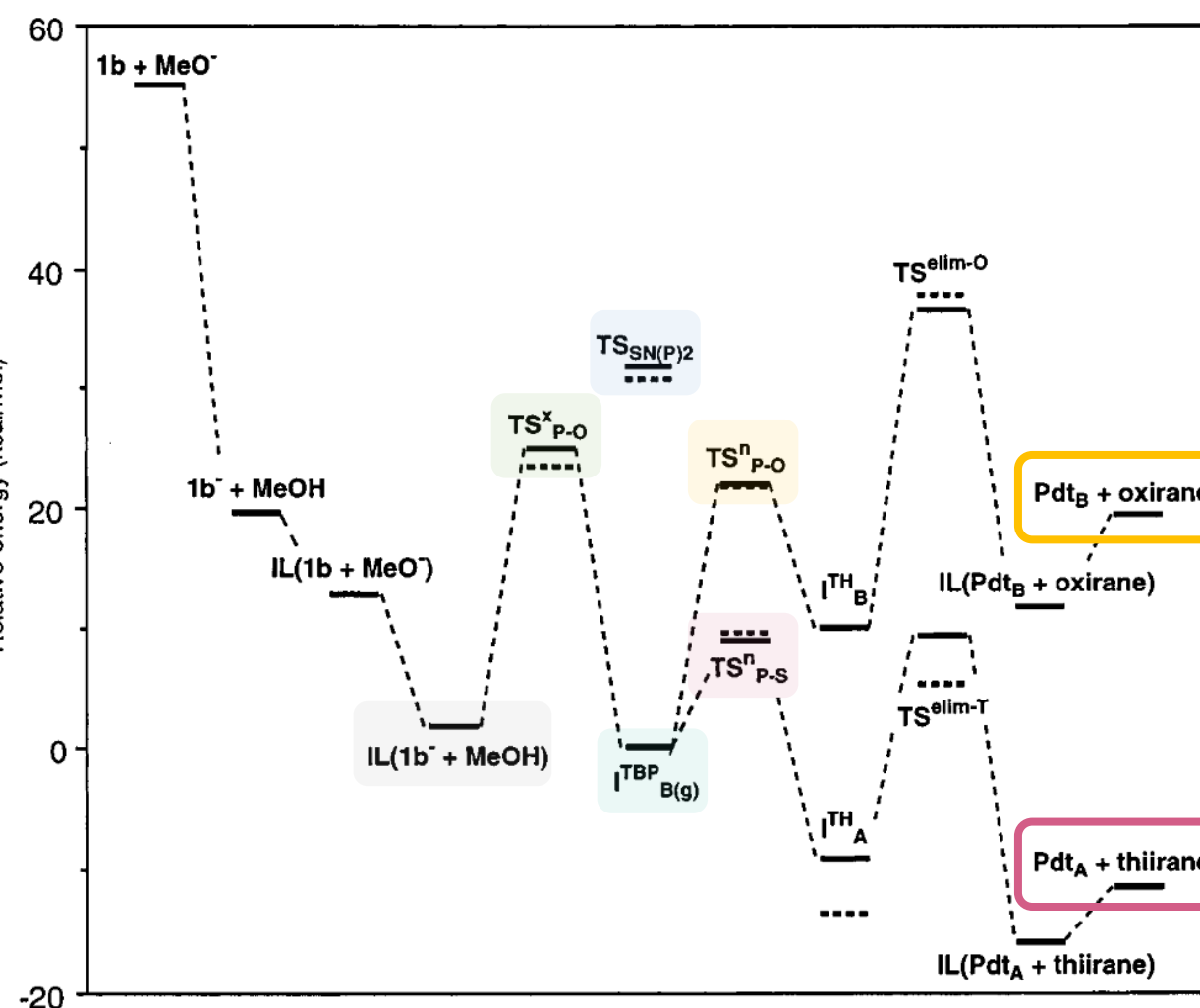
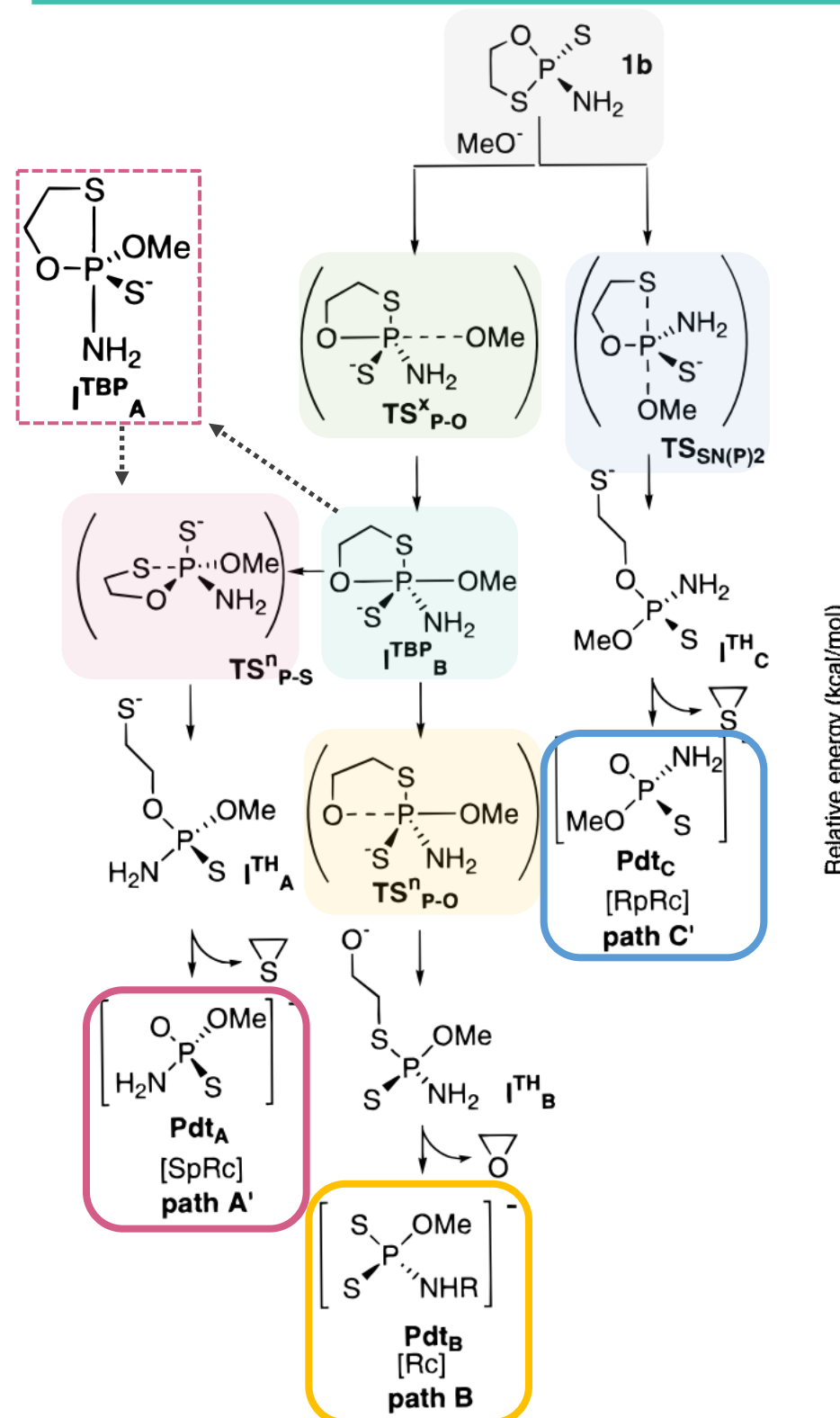
- $\text{I}^{\text{TBP}}_{\text{A}}$ is unstable compared with $\text{I}^{\text{TBP}}_{\text{B}} \dots$
(S and N are less apicophilic than O)
- The elimination of **equatorial ligand** doesn't occur directly...

Why does the substitution occur in such a way?

Ab initio calculation

^a ψ indicates a pseudorotation process.

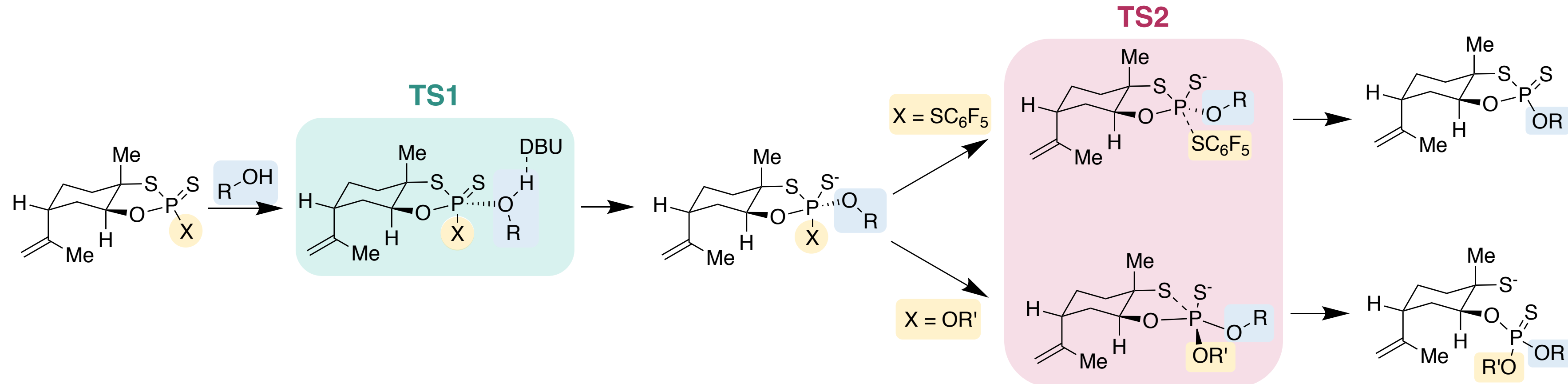
Ab initio calculation



1. Nucleophilic attack of methoxide collinear to the endocyclic P–S bond should occur in concert with breaking of the P–S bond. (Path C)
2. Pseudorotation in ITBP_B will occur concomitant with cleavage of the endocyclic P–S bond via the transition state $\text{TS}_{\text{P-S}}^n$ to immediately give IT_A^{H} , without forming ITBP_A . (Path A)
3. Path A will be preferred over either path B or C.

^a The transition-state structures are shown in parentheses.

Answer: The stereochemistry of ψ reagents



- Nucleophilic attack of alcohol will occur from the opposite side of endocyclic oxygen via **TS1**.
- Pseudorotation will occur accompanied by the cleavage of the endocyclic P–S bond via **TS2**.
- These processes lead to the diastereoselective reaction with **a retention of configuration** at phosphorus.

Uchimaru, T.; Stec, W.; Taira K. *J. Org. Chem.*, **1997**, *62*, 5793

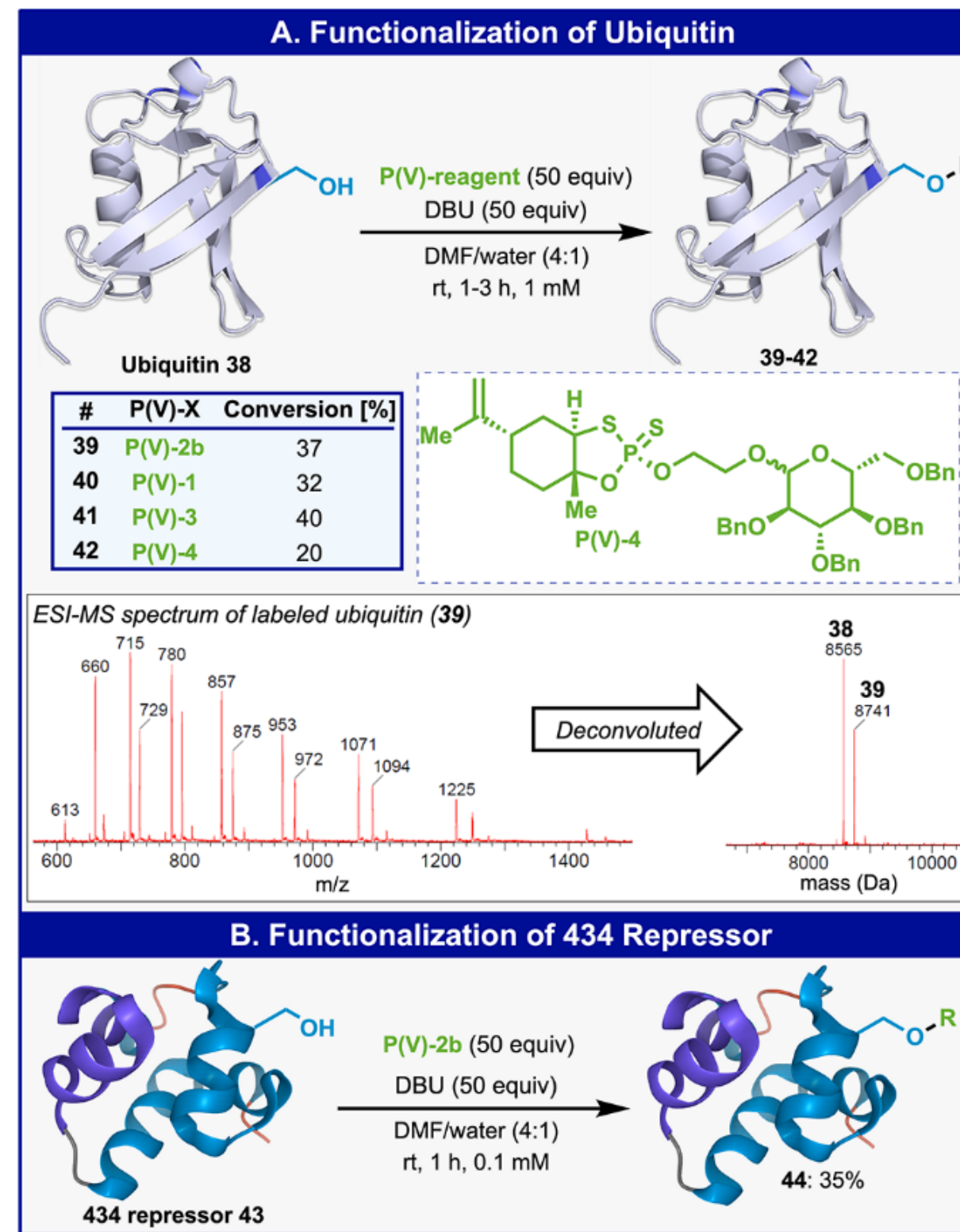
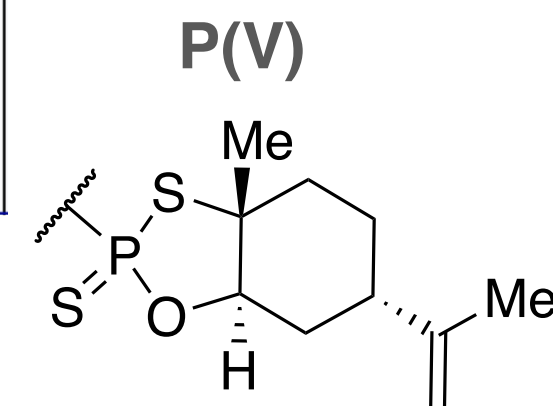
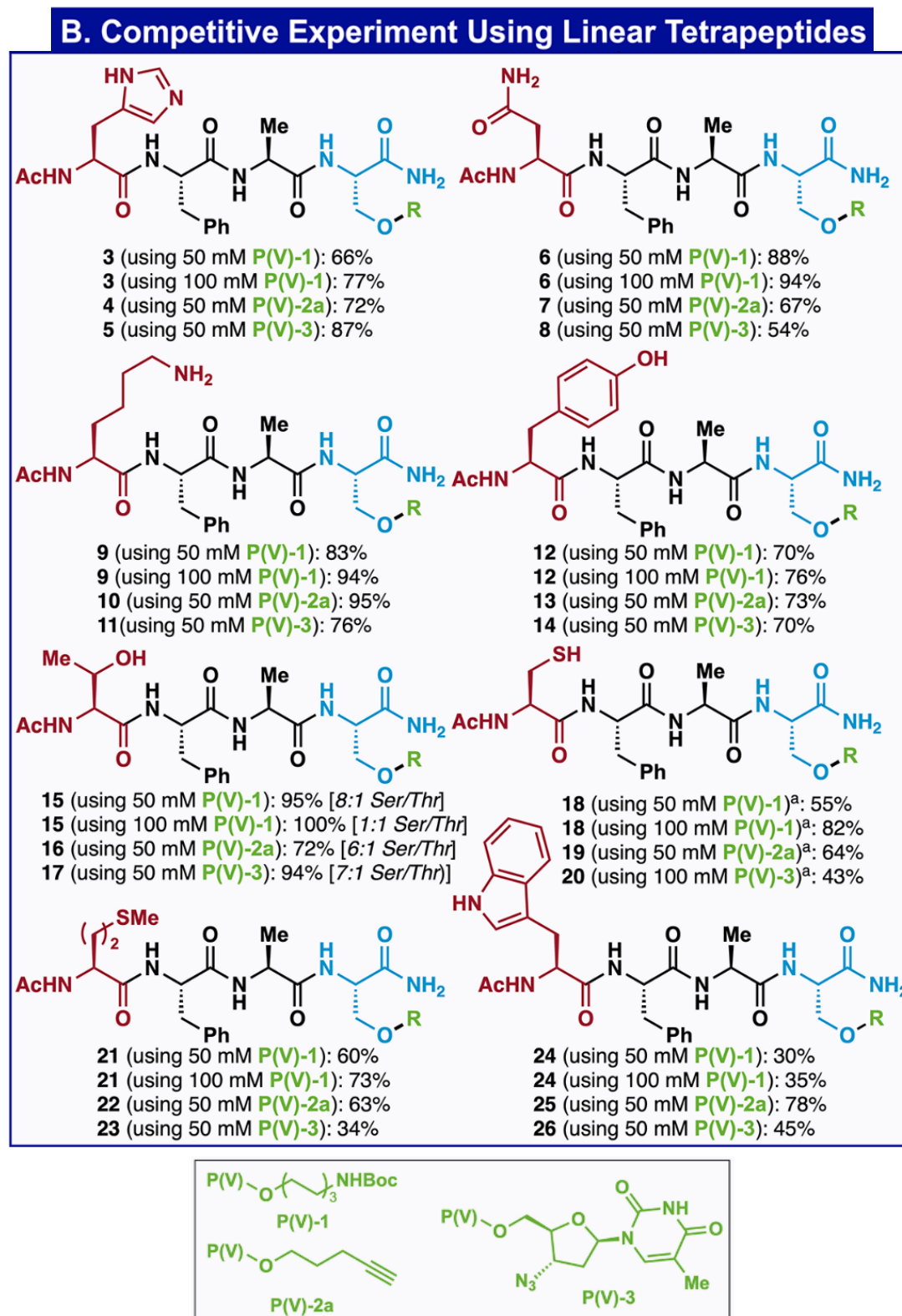
Knouse, K. W.; Baran, P.; et al. *Science*, **2018**, *361*, 1234

Vantourout, J.; Baran, P.; et al. *J. Am. Chem. Soc.* **2020**, *142*, 17236

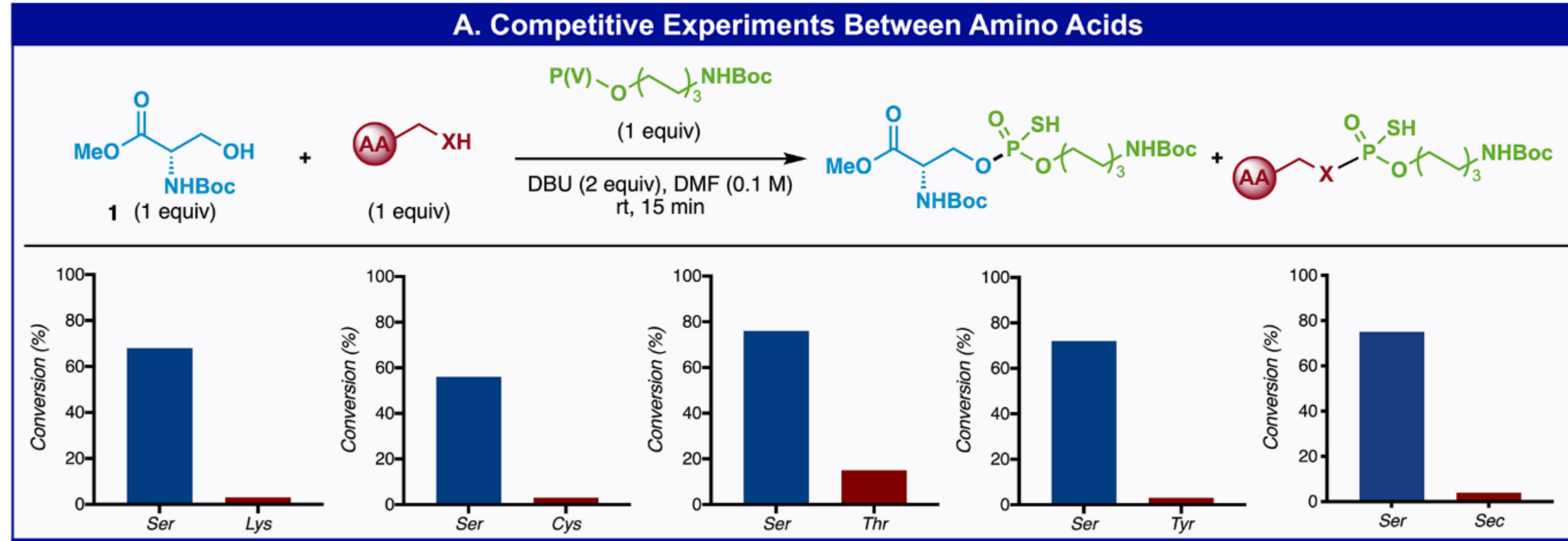
The noteworthy points of ψ reagent

- **Stereoselectivity**
 - *d.r.* >99:1 in the synthesis of ASO
- **Chemosselectivity**
 - Serine-selective phosphorylation in the presence of other nucleophiles
- **High reactivity under mild condition**
 - 30 min at r.t. in loading and coupling reaction

Serine selective bioconjugation



Question: The chemoselectivity of ψ reagent

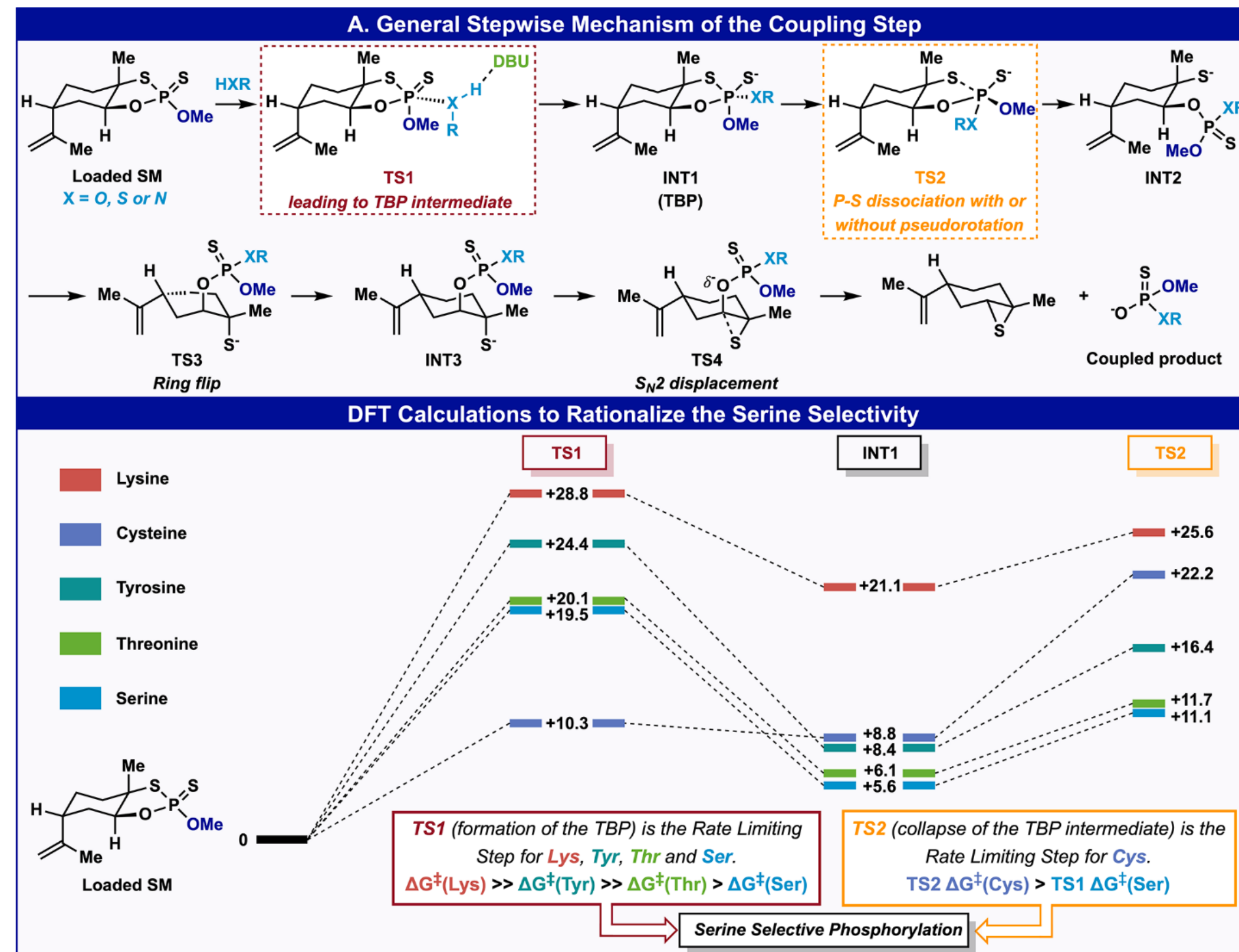


ψ reagent selectively react with serine-OH in the presence of other nucleophiles.

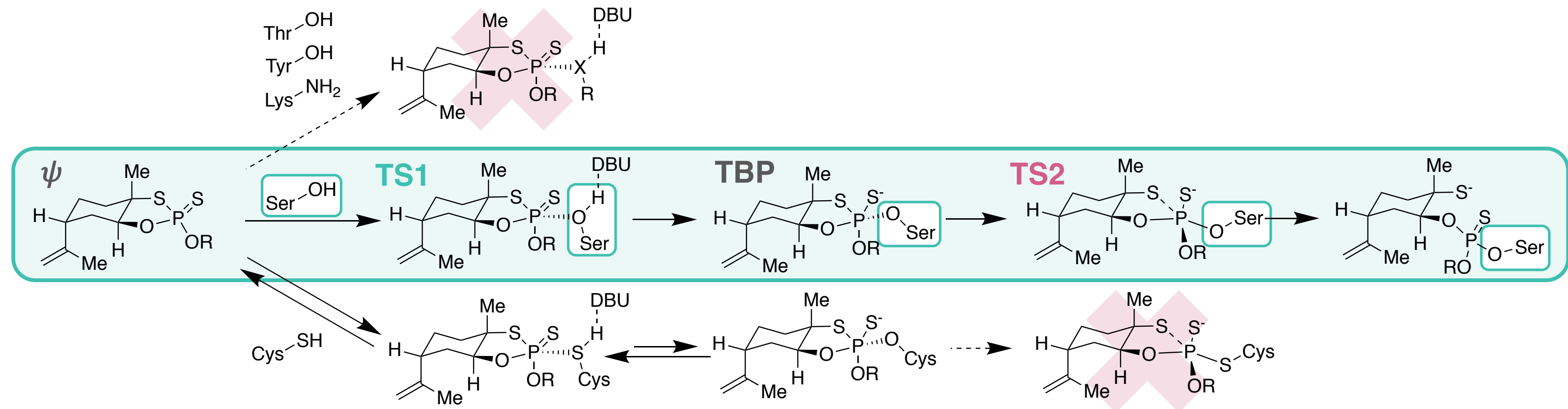


How does ψ reagents distinguish nucleophiles?

DFT calculations to rationalize the serine selectivity



Answer: The chemoselectivity of ψ reagent



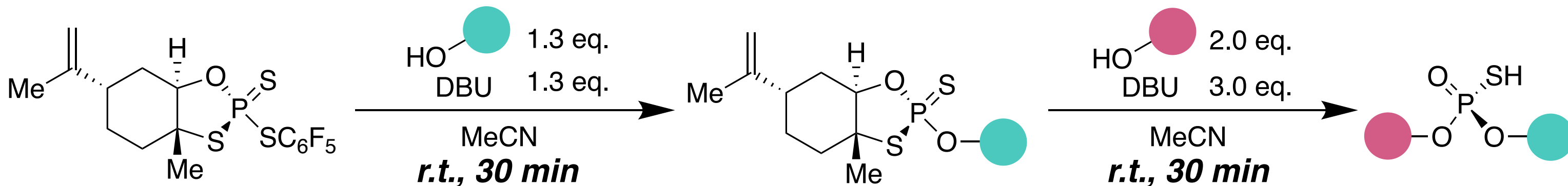
- Barriers in the formation of TBP intermediate (**TS1**)
 $\text{Cys} \ll \text{Ser} < \text{Thr} < \text{Tyr}$ (limited reactivity) $\ll \text{Lys}$ (lower acidity of primary amine)
- For **Cys**, the collapse of the TBP intermediate is late limiting step.
 $\Delta G^\ddagger (\text{Cys}) > \Delta G^\ddagger (\text{Ser})$
- These results rationalize the serine selectivity.

The noteworthy points of ψ reagent

- **Stereoselectivity**
 - *d.r.* >99:1 in the synthesis of ASO
- **Chemoselectivity**
 - Serine-selective phosphorylation in the presence of other nucleophiles
- **High reactivity under mild condition**
 - 30 min at r.t. in loading and coupling reaction

Question: The best reactivity of ψ reagent

Bench stable



Knouse, K. W.; Baran, P.; et al. *Science*, 2018, 361, 1234

ψ reagent has great stability for air and moisture and is highly reactive under mild condition.

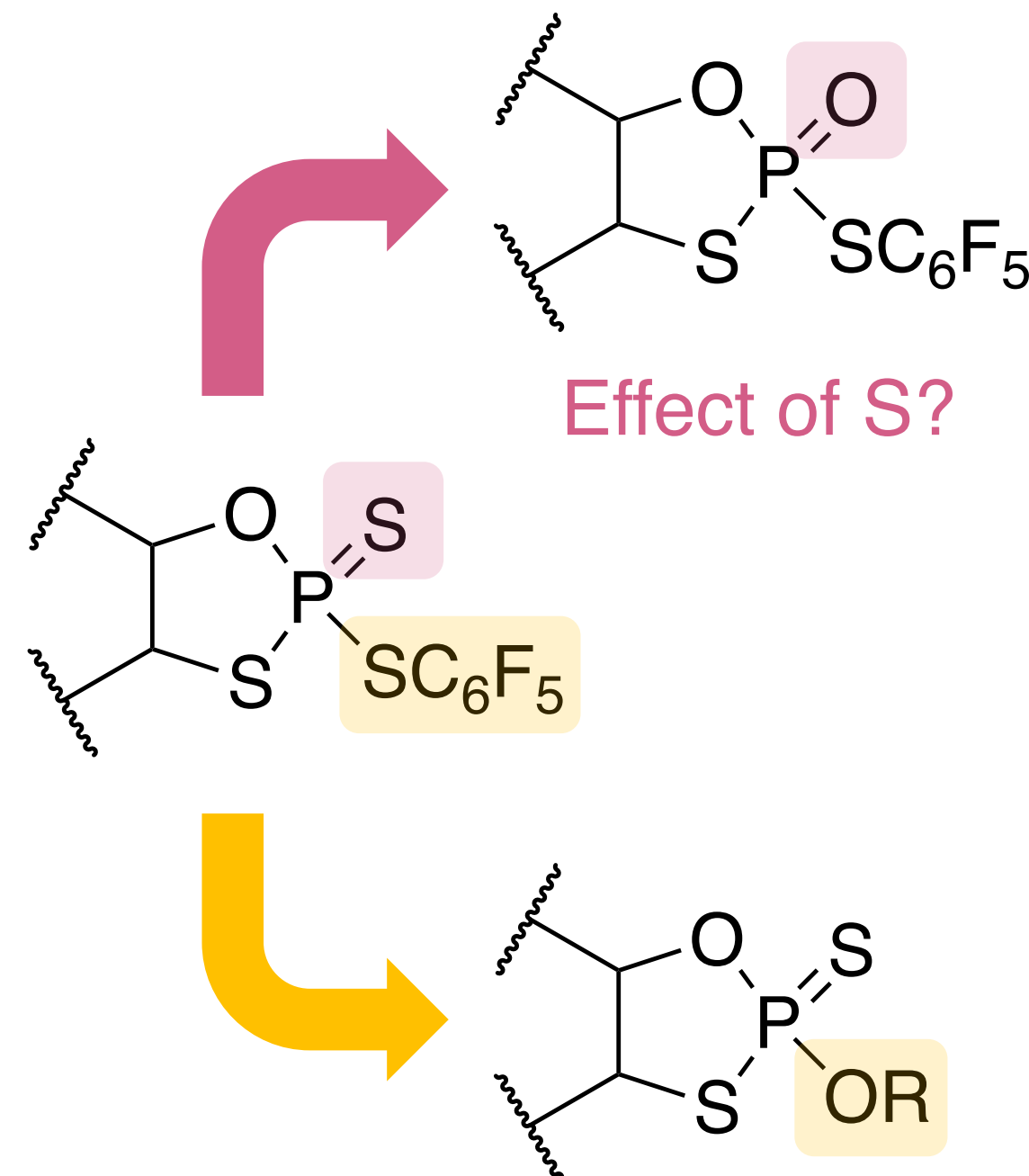


How does ψ reagent realize the balance of stability and reactivity?

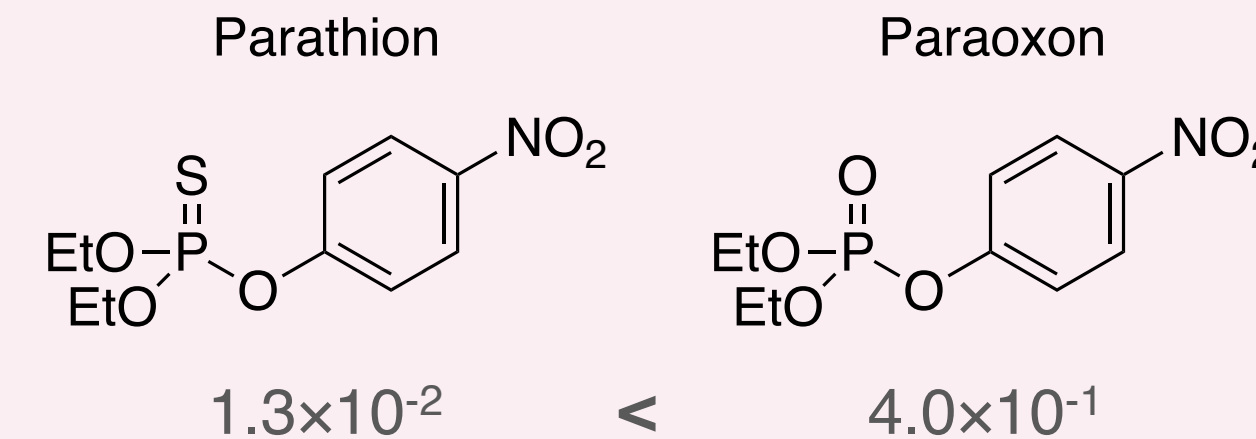
DBU is one of the most effective base for activation of alcohol.

However, is the effect of base only a reason for the high reactivity?

What is the key structure for high reactivity?



Effect of leaving group?



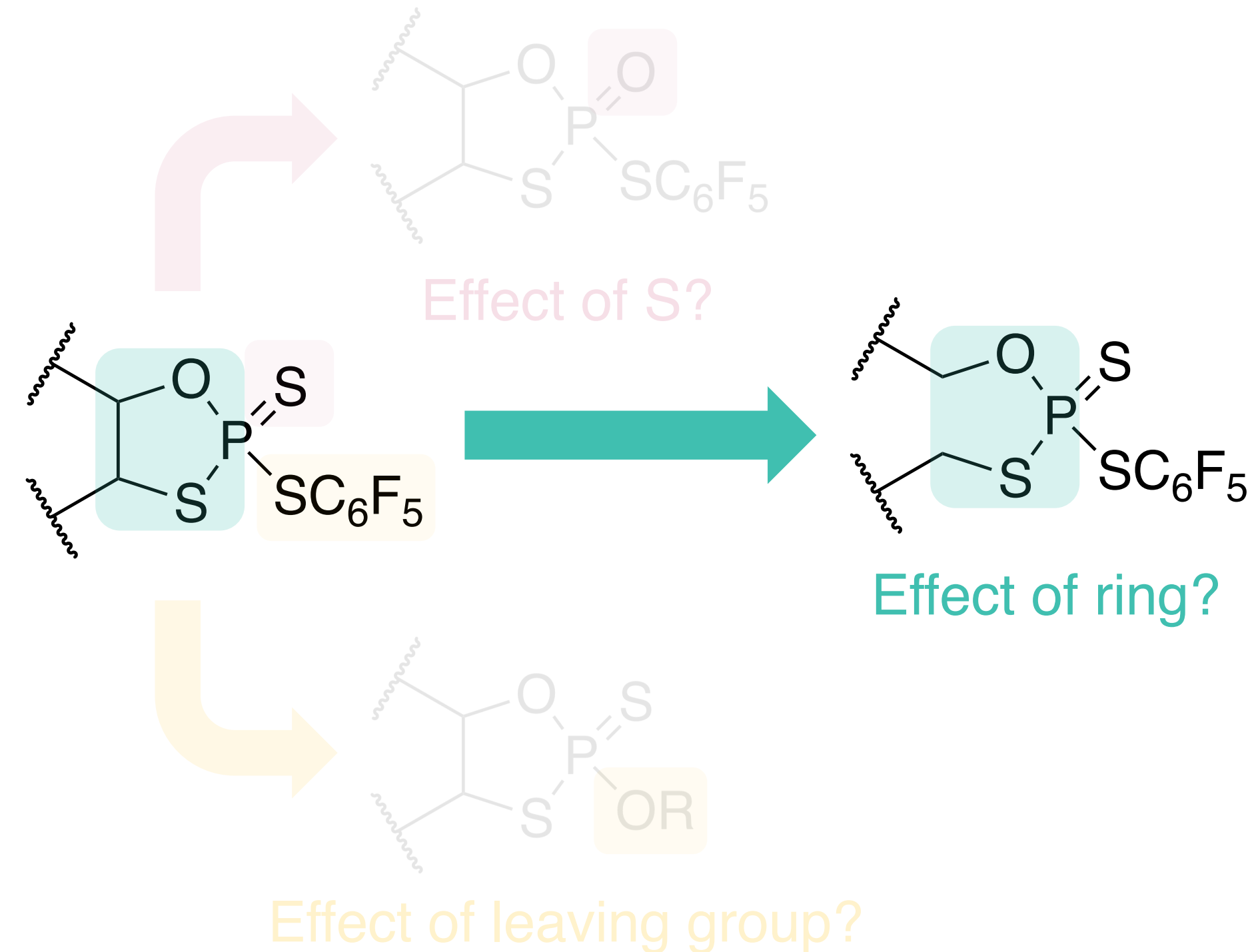
Ketelaar, J.A.A. and Gersmann, H.R. *Recl. Trav. Chim. Pays-Bas.* **1958**, *77*, 973

The reactions in both of the loading and coupling steps finished in **30 min at r.t.**

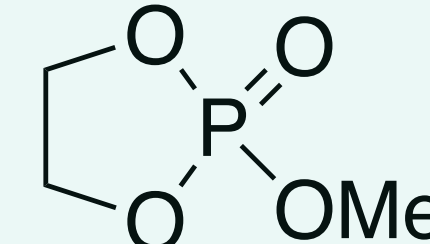
→ The leaving group should not be critical for high reactivity.

Knouse, K. W.; Baran, P.; et al. *Science*, 2018, 361, 1234

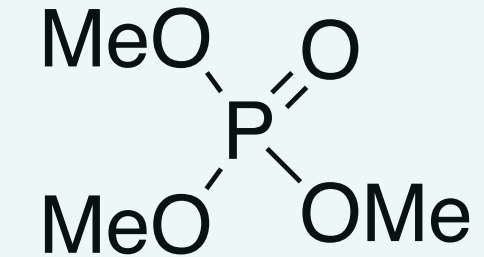
The answer lies in ring moiety



Which is faster for hydrolysis?

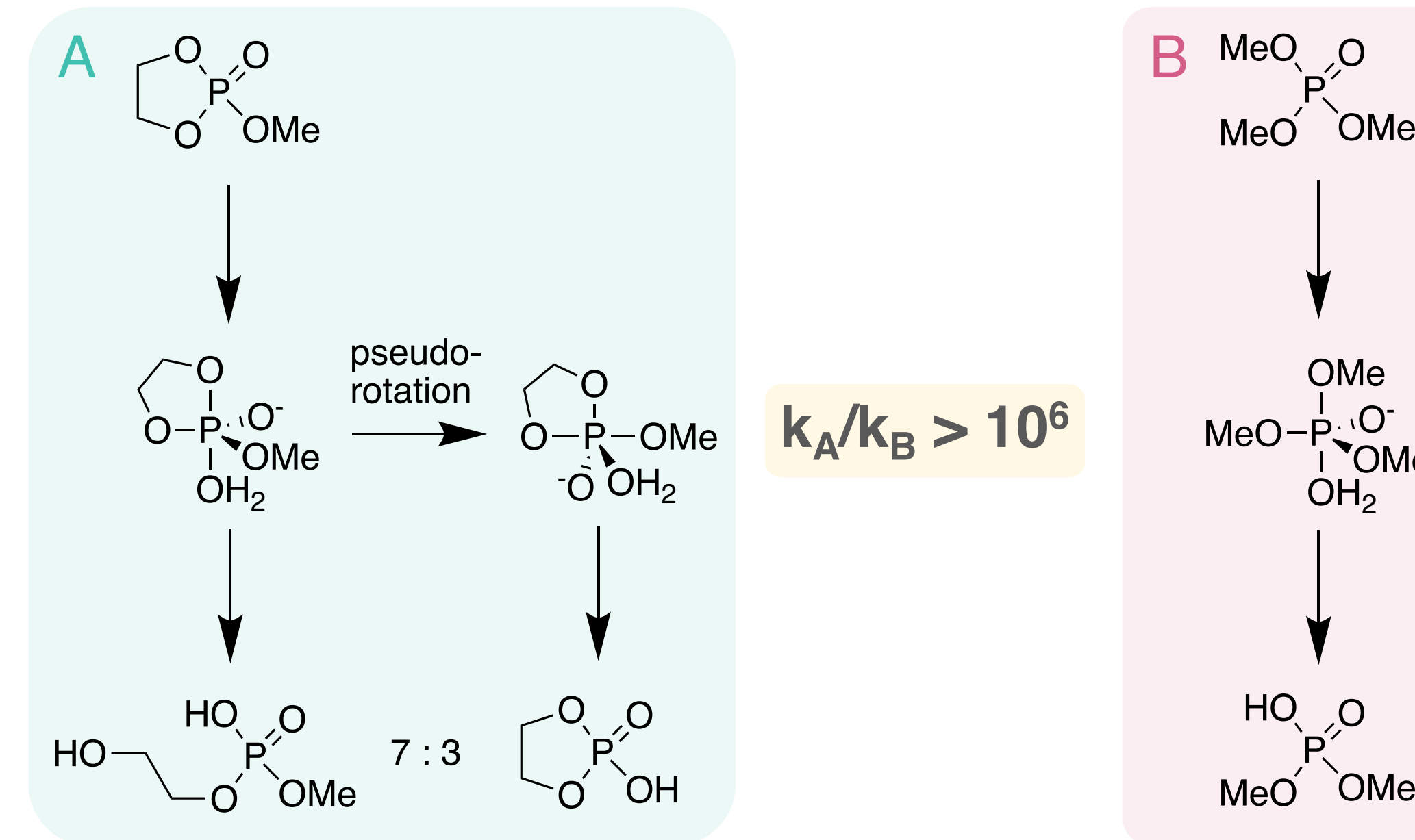


vs.



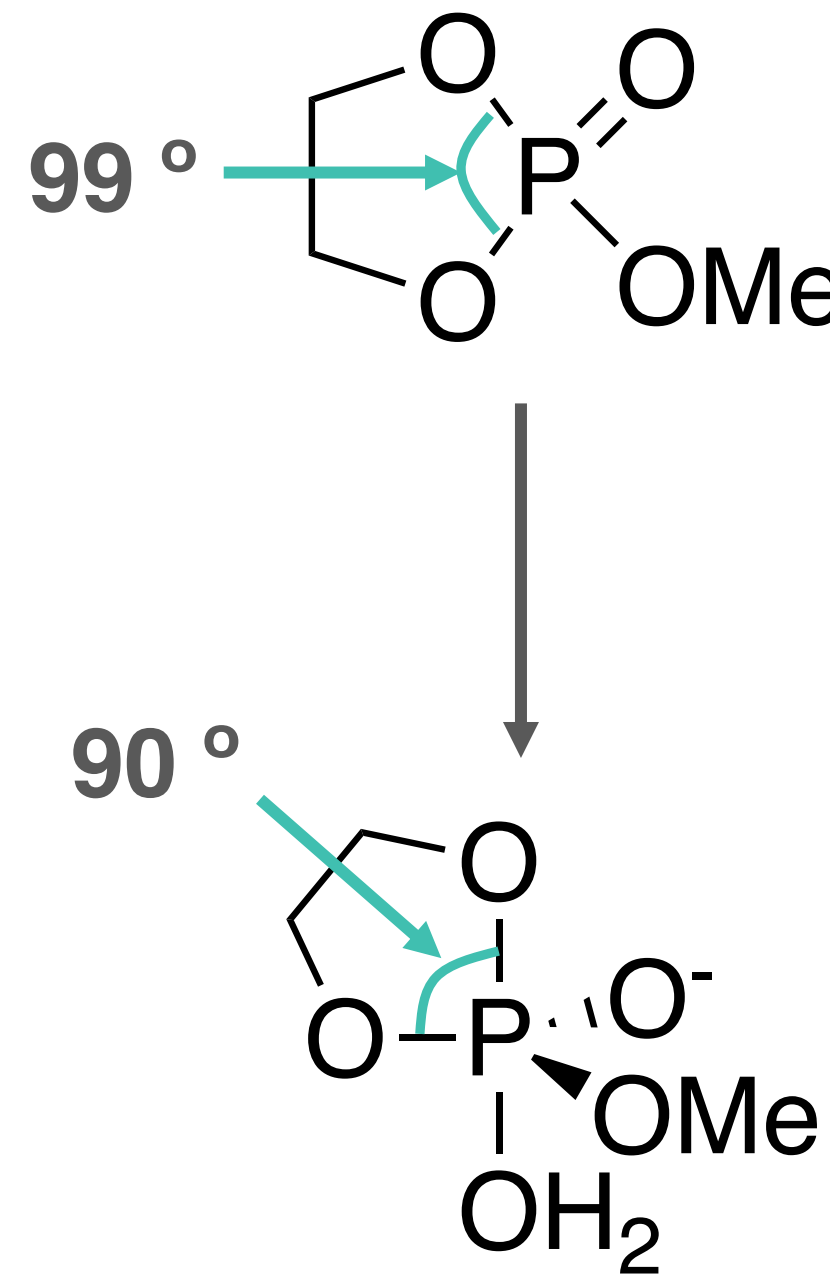
Westheimer, F. H. *Acc. Chem. Res.* **1968**, 1, 70

The rate of hydrolysis: Five-membered ring vs. acyclic phosphate



The rate of hydrolysis of methyl ethylene phosphate **A** (k_A) exceeds that of trimethyl phosphate **B** (k_B) by 10^6 .

TBP intermediate of five-membered ring phosphate in hydrolysis

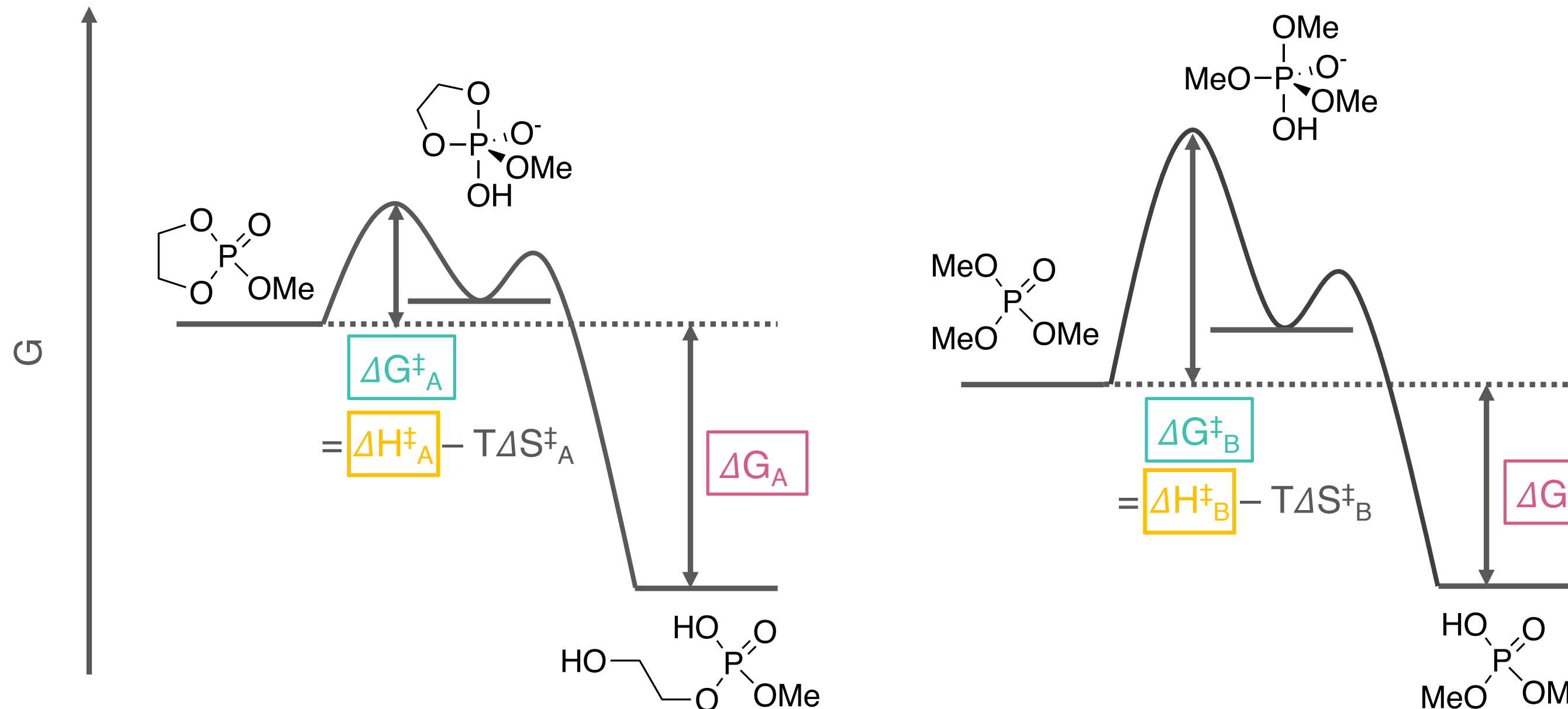


The ring angle at phosphorus (O-P-O) is **99 °** determined by X-ray crystallography.

The five-membered ring is **highly strained**.

The formation of the TBP intermediate with a **90 °** angle at phosphorus (ring in the **equatorial–apical** conformation) **largely decrease the strain energy**.

Driving force: ring strain

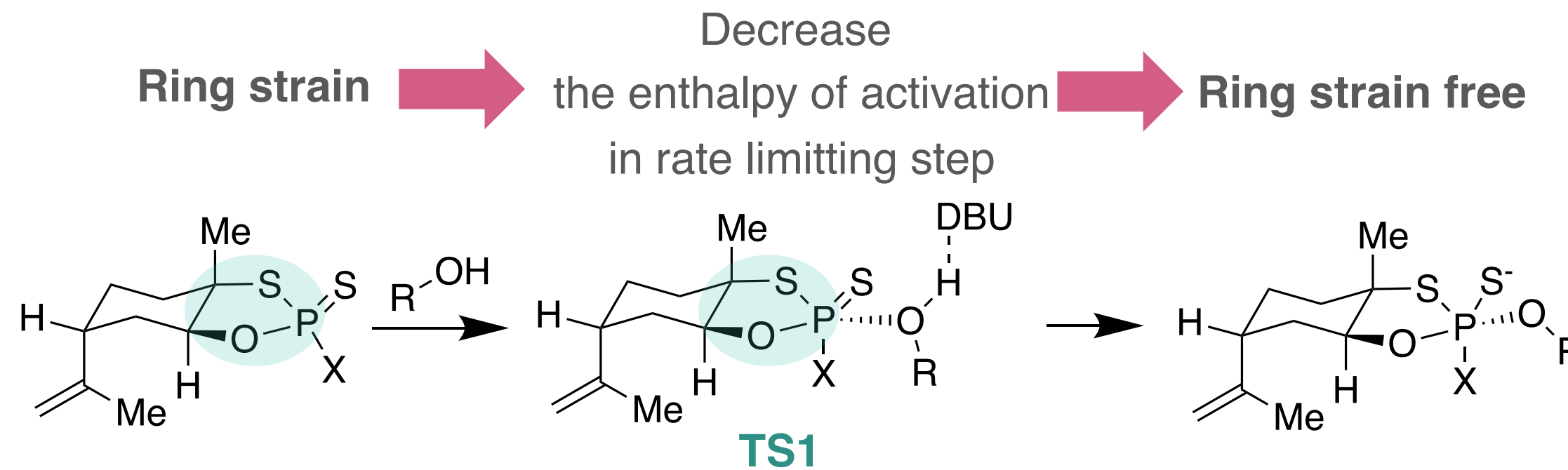


$$\begin{aligned}\Delta G_A - \Delta G_B &= 5\text{--}6 \text{ kcal/mol} \\ \Delta G^\ddagger_A - \Delta G^\ddagger_B &= -8.5 \text{ kcal/mol} \\ \Delta H^\ddagger_A - \Delta H^\ddagger_B &= -7.6 \text{ kcal/mol}\end{aligned}$$

The difference of ΔH^\ddagger is comparable to that of ΔG^\ddagger .

The release of ring strain accounts for the rapid hydrolysis of five-membered ring phosphate A compared with acyclic one B.

Answer: The best reactivity of ψ reagent

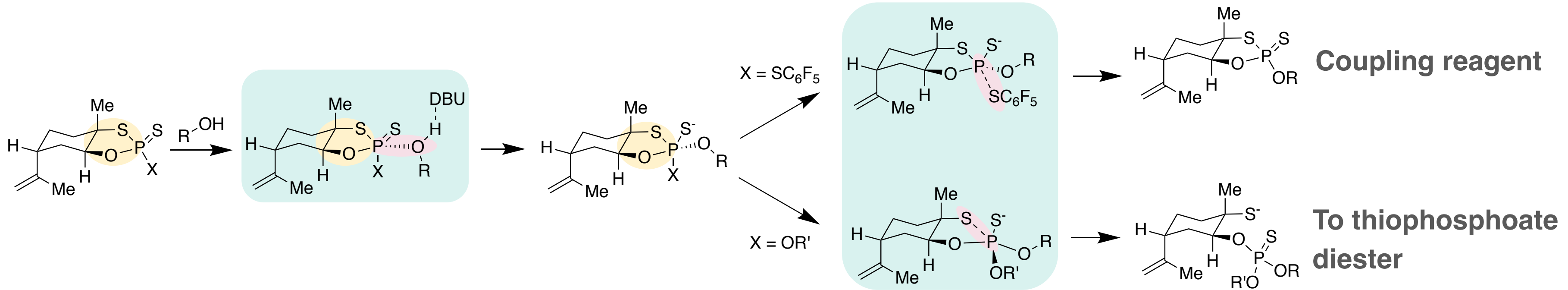


The driving force of ψ reagent should be **the ring strain**.

It should decrease the activation energy compared with acyclic phosphate.

This is why ψ reagent shows the high reactivity.

Summary



Stereoselectivity

- 1) The direction of nucleophilic addition
- 2) The cleavage of P–S bond accompanied by pseudorotation

Chemosselectivity

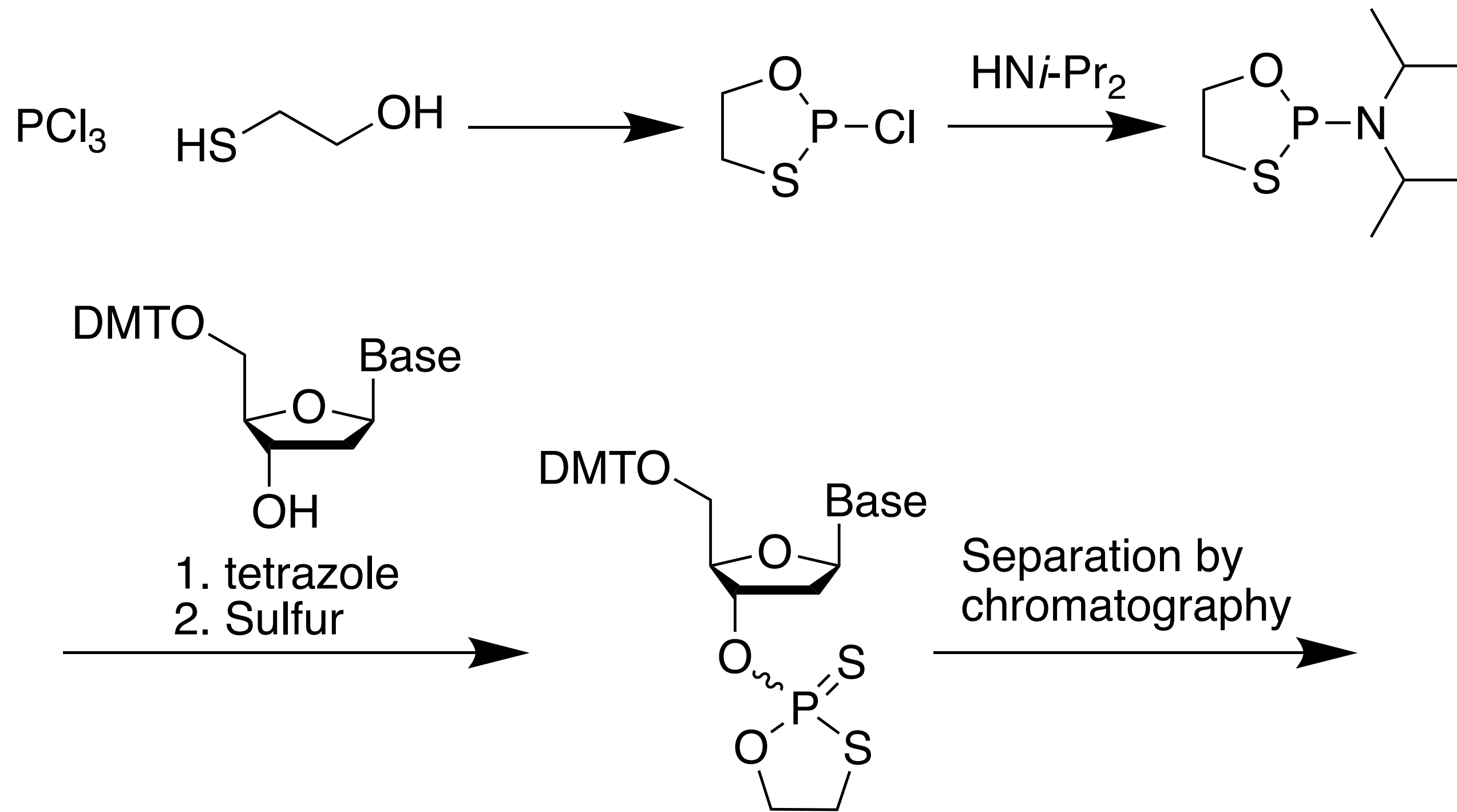
- 1) ΔG^\ddagger in TS1
Cys << Ser
< Thr << Tyr << Lys
- 2) TS2 ΔG^\ddagger (Cys)
> TS1 ΔG^\ddagger (Ser)

High reactivity

- 1) Strained five membered ring
- 2) Lower the enthalpy of the activation in TS1

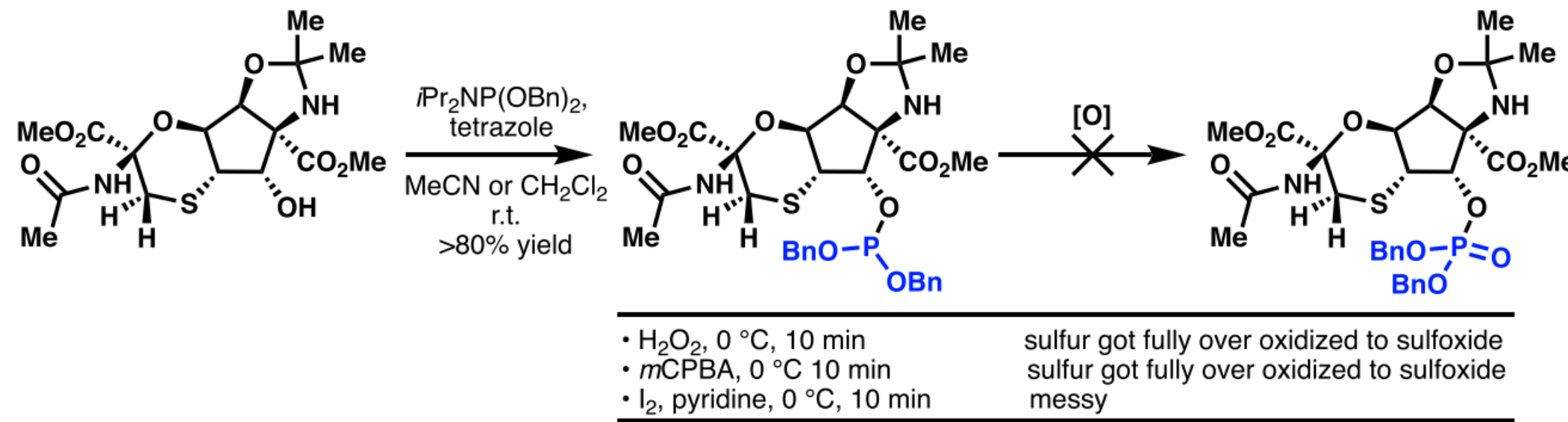
Appendix

Appendix: Synthesis of 5'-O-DMT-nucleoside 3'-O-(2-thio-1,3,2-oxathiaphospholane)

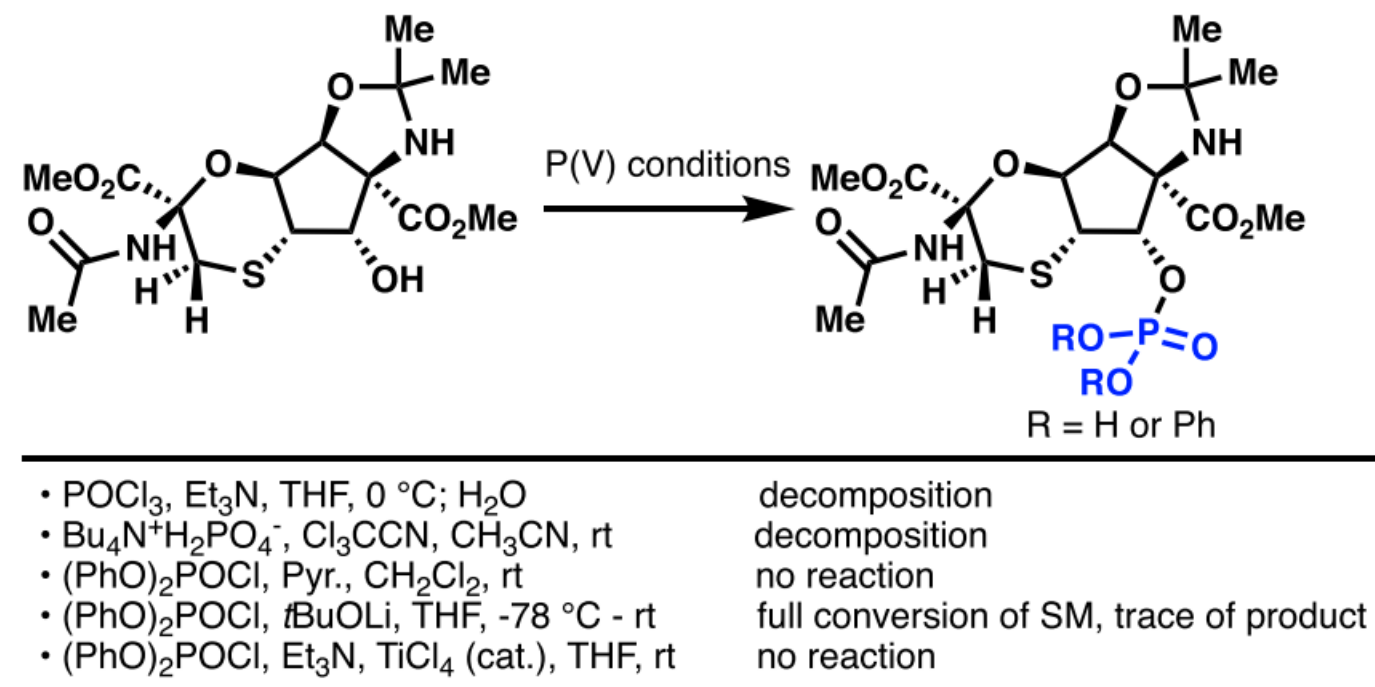


Appendix: Phosphorylation of existing method

a) P(III) to P(V) strategy: Oxidation was difficult to control. S tends to get over oxidized.



b) Conventional P(V) strategy: conditions were either too harsh or invalid.

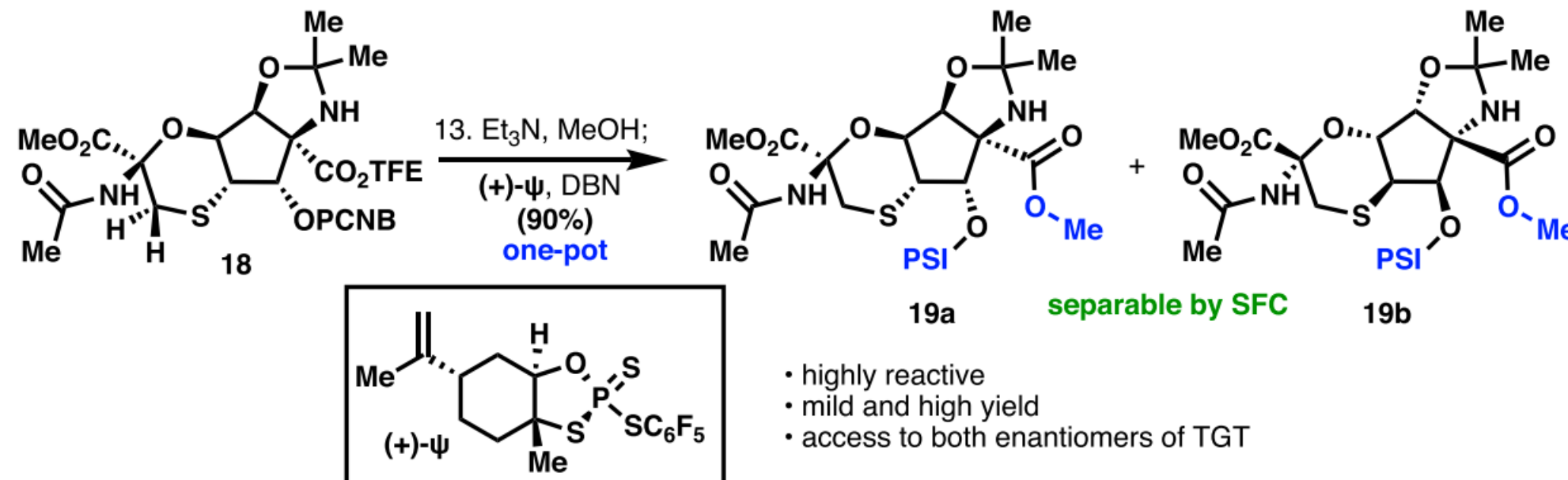


The introduction of phosphoryl group to a secondary alcohol by existing methods was quite difficult.

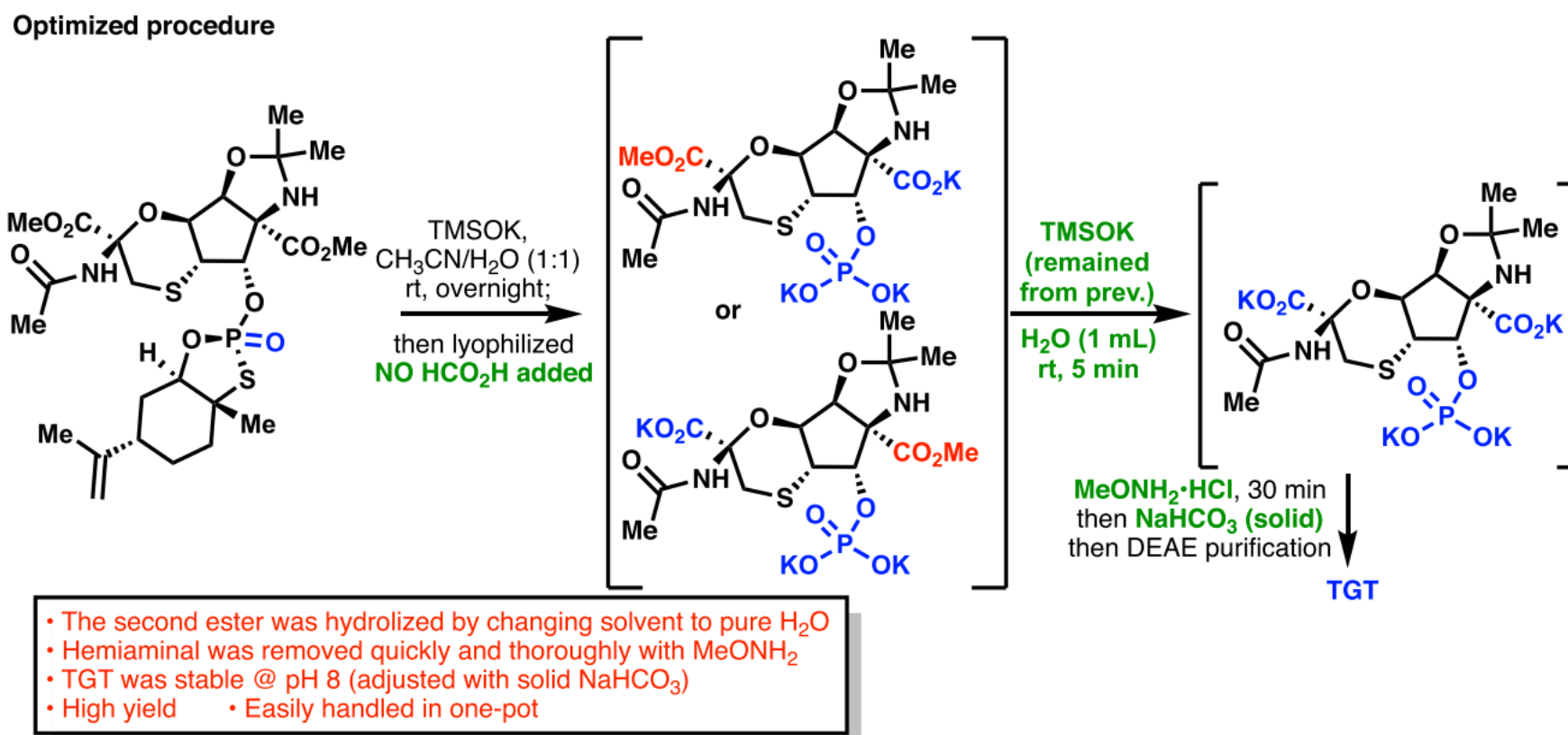
- Phosphoramidite
 - Sulfide was oxidized...
- Other reagents
 - Too harsh or invalid...

Appendix: Phosphorylation by Ψ reagent

c) Final phosphorylation with (+)- Ψ :



Scheme S20. Optimization of phosphorylation



Ψ reagent provided thiophosphate triester in high yield (90%).

SeO_2 oxidation and hydrolysis of phosphate thioester gave a phosphomonoester final product Tagetitoxin.

Appendix: The rate of hydrolysis of some phosphorus acid esters

976

J. A. A. Ketelaar and H. R. Gersmann,

Chemical studies on insecticides IV.

77 (1958) RECUEIL 977

No.	Compound	Solvent	log. freq. factor (min ⁻¹)	Acti- vation Energy cal/mole	Results of hydrolysis measurements					
					Acti- vation Entropy (Entr. Units)	Free Energy of Acti- vation cal/mole	k(25° C) min ⁻¹ mole ⁻¹	k(37.5° C) min ⁻¹ mole ⁻¹	Inhibition Cholinesterase* I ₅₀	I ₅₀ Ali-esterase*) I ₅₀ Cholinesterase
1	(C ₂ H ₅ O) ₃ PO	H ₂ O	7.94	15000	-32.2	24100	7.9 × 10 ⁻⁴	2.24 × 10 ⁻³	> 10 ⁻¹	—
2	(C ₂ H ₅ O) ₂ (C ₆ H ₅ O)PO	50 % ethanol	8.76	15000	-28.5	23900	5.3 × 10 ⁻³	1.48 × 10 ⁻²	10 ⁻³	3
3	(C ₂ H ₅ O) ₂ (p-O ₂ NC ₆ H ₄ O)PO	50 % acetone	8.64	12400	-29.0	20500	4.0 × 10 ⁻¹	9.5 × 10 ⁻¹	10 ⁻⁸	20
4	(C ₂ H ₅ O) ₂ (m-[N ⁺ (CH ₃) ₃]C ₆ H ₄ O)PO	50 % ethanol	11.90	15800	-14.2	19500	1.86	5.5	8 × 10 ⁻⁹	5 × 10 ⁻⁶
5	(C ₂ H ₅ O)(p-O ₂ NC ₆ H ₄ O) ₂ PO	50 % acetone	11.96	14300	-13.9	17900	3.1 × 10	8.2 × 10	2 × 10 ⁻⁸	10
6	(CH ₃ O)(p-O ₂ NC ₆ H ₄ O) ₂ PO	50 % acetone	11.25	13400	-17.2	17900	3.4 × 10	7.8 × 10	4 × 10 ⁻⁸	5
7	(p-O ₂ NC ₆ H ₄ O) ₂ P(O)OH	20 % ethanol	10.01	18300	-22.8	24500	3.5 × 10 ⁻⁴	1.2 × 10 ⁻³		
8	(p-O ₂ NC ₆ H ₄ O) ₂ C ₂ H ₅ PO	20 % ethanol	8.97	8700	-27.5	16400	3.7 × 10 ²	6.8 × 10 ²	5 × 10 ⁻⁷	0.14
9	(C ₆ H ₅ O) ₃ PO	75 % ethanol	13.57	16100	-6.6	17500	5.4 × 10	1.6 × 10 ⁻²	> 10 ⁻²	< 0.15
10	(p-O ₂ NC ₆ H ₄ O) ₃ PO	50 % acetone	6.34	4100	-39.6	15400	2.0 × 10 ³		4 × 10 ⁻⁶	1
11	p-ClC ₆ H ₄ OP(O)(NHC ₂ H ₅) ₂	50 % ethanol	10.85	16700	-19.0	21800	3.6 × 10 ⁻²	1.1 × 10 ⁻¹	10 ⁻²	3 × 10 ⁻³
12	(p-ClC ₆ H ₄ O) ₂ P(O)NHCH ₃	50 % ethanol	12.01	15200	-13.7	18700	6.8	1.9 × 10	1.5 × 10 ⁻³	1.4 × 10 ⁻³
13	(CH ₃ O) ₂ (p-O ₂ NC ₆ H ₄ O)PS	50 % acetone	11.26	16700	-17.1	21200	8.5 × 10 ⁻²	3.4 × 10 ⁻¹	5 × 10 ⁻⁴	0.8
	"	H ₂ O	10.76	15450	-19.6	20700				
14	(C ₂ H ₅ O) ₂ (p-O ₂ NC ₆ H ₄ O)PS	50 % acetone	11.96	19200	-13.9	22700	1.3 × 10 ⁻²	5.5 × 10 ⁻²	(?) 2.5 × 10 ⁻⁵	1.5
	"	H ₂ O	10.95	16600	-18.5	21600				
15	(C ₂ H ₅ O)(p-O ₂ NC ₆ H ₄ O)C ₆ H ₅ PS	20 % ethanol	13.79	17500	-5.6	18600	9.1	2.7 × 10		
16	(p-O ₂ NC ₆ H ₄ O) ₂ (C ₂ H ₅ O)PS	50 % acetone	8.73	12100	-28.6	20100	9.7 × 10 ⁻¹	1.8	4 × 10 ⁻³	0.25
17	(p-O ₂ NC ₆ H ₄ O) ₂ (CH ₃ O)PS	50 % acetone	10.33	13900	-21.3	19700	1.35		1 × 10 ⁻³	
18	(p-O ₂ NC ₆ H ₄ O) ₃ PS	50 % acetone	5.21	5700	-44.7	18500	1.25 × 10		2 × 10 ⁻⁴	0.5
19	(CH ₃ O) ₂ [(CO ₂ C ₂ H ₅) ₂ CH ₂ CH]S)PS	25 % acetone	20.45	24500	-24.75	16500	2.6 × 10 ²	1.4 × 10 ³	(?) 5 × 10 ⁻⁶	15

*) These values were taken from the work of Mendel and Myers⁹.

Appendix: Ab initio calculations for MEP vs. TMP or EPP

Table 7. Experimental Activation Parameters (kcal/mol) for the Alkaline Hydrolyses of Acyclic TMP, Five-Membered Ring MEP, and 6-Membered Ring EPP at 298.15 K

molecule	ΔH^\ddagger	$T\Delta S^\ddagger$	ΔG^\ddagger
TMP ^a	15.60 ± 0.2	-6.86 ± 0.3	22.46 ± 0.3
MEP ^a	7.80 ± 0.2	-6.86 ± 0.3	14.66 ± 0.3
EPP ^b	13.21	-8.74	21.94
TMP-MEP	7.8 ± 0.4	0.00 ± 0.6	7.80 ± 0.6
EPP-MEP	5.4 ± 0.4	-1.88 ± 0.6	7.29 ± 0.6

^a Values are taken from ref 12. ^b Values are taken from ref 16. No errors were reported for the activation parameters obtained.

Table 8. Intra- and Intermolecular Contributions to the Rate Acceleration of Five-Membered Ring MEP Relative to Its Acyclic and Six-Membered Ring Analogs (All Energies Are Reported to 1 Decimal Place in kcal/mol)

a	TMP-MEP			MPP-MEP		
	b,d	c,d	c,e	b,d	c,d	c,e
$\Delta\Delta E^\ddagger$	-5.8	-3.8	-4.2	2.3	1.8	2.5
$\Delta\Delta\delta E^\ddagger(T)$	1.1	1.1	1.1	0.2	0.2	0.2
$\Delta(T\Delta S^\ddagger)$	-1.3	-1.3	-1.3	-1.1	-1.1	-1.1
$\Delta\Delta G_{\text{gas}}^\ddagger$	-3.3	-1.3	-1.8	3.6	3.1	3.8
$\Delta\Delta G_s(\text{TS})$	11.1	10.7	16.4	-1.2	3.1	3.5
$\Delta\Delta G_s(\text{GS})$	1.3	1.3	2.5	0.3	0.3	0.7
$\Delta\Delta G_{\text{sln}}^\ddagger$	6.5	8.1	12.2	2.1	5.9	6.6

^a Ground state to rate-limiting transition state. ^b Energies and free energies corresponding to gas-phase rate-limiting transition state.

^c Energies and free energies corresponding to relocated rate-limiting transition state in solution. ^d Solvation free energies computed using the continuum dielectric method. ^e Solvation free energies computed using combined PSGVB/DelPhi programs.

Appendix: Ab initio calculations for MEP vs. TMP or EPP

Scheme 1. Schematic Diagram Depicting Fully Optimized HF/6-31+G* Structures for the Reaction of $(\text{OH})^-$ at the Phosphorus of TMP (TMP(P)) (Not All Transition States and Intermediates along the Pathways Are Depicted for the Sake of Clarity.)

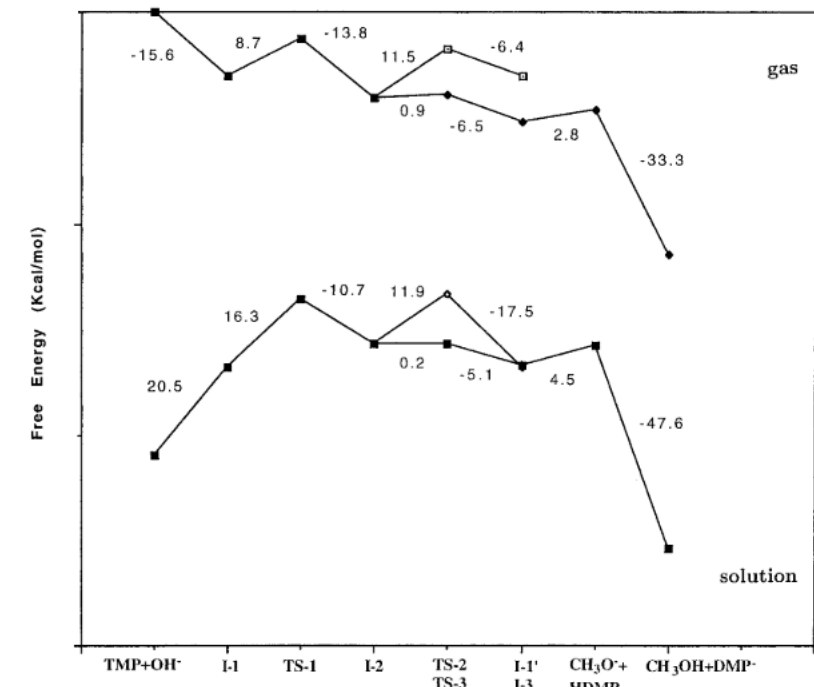
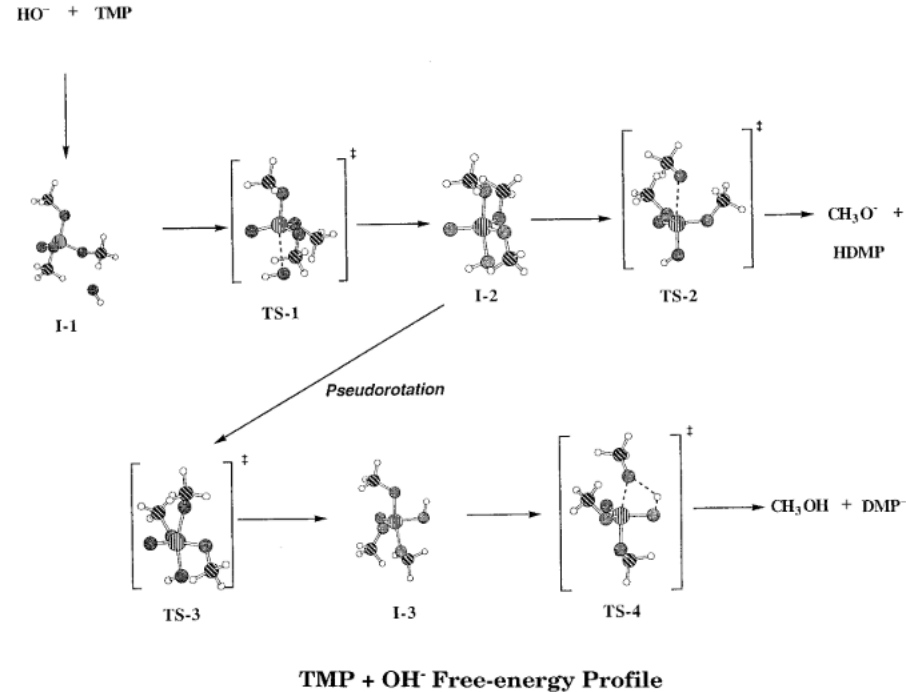


Figure 1. Relative MP2/6-31+G*/HF/6-31+G* activation free-energy profile for the gas-phase reaction of $(\text{OH})^-$ with TMP (top) and the change in profile upon solvation (bottom). The zero of energy corresponds to the reactants at infinite separation. The numbers correspond to the free-energy differences of subsequent points. The free energy of the ion-dipole complex, $(\text{CH}_3\text{O})^-\cdots\text{HDMP}$, which was not computed, was assumed to be similar to that of I-1.

Scheme 2. Schematic Diagram Depicting Fully Optimized HF/6-31+G* Structures for the Reaction of $(\text{OH})^-$ at Phosphorus of MEP (MEP(P)) (Not All Transition States and Intermediates along the Pathways Are Depicted for the Sake of Clarity.)

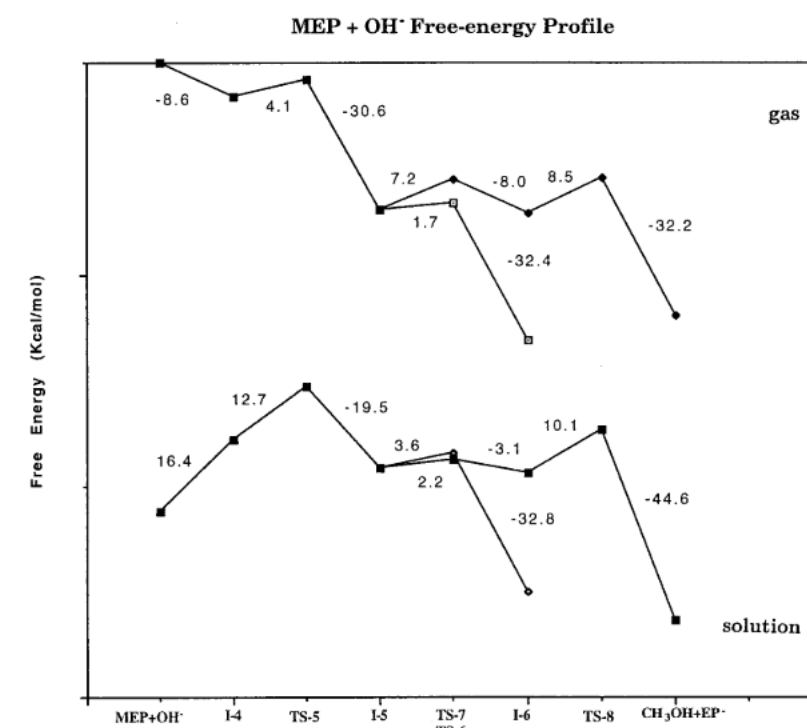
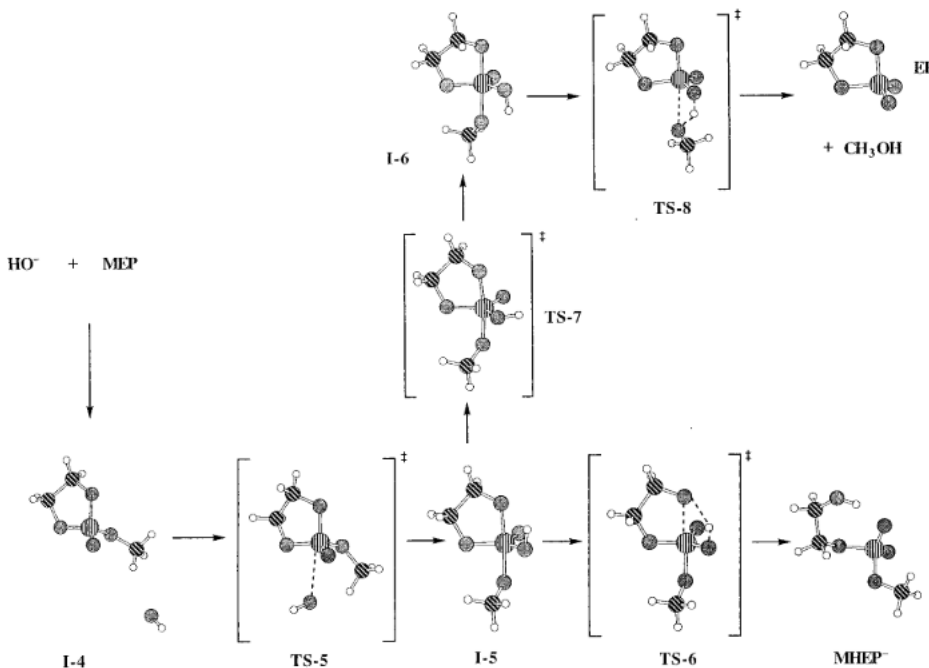


Figure 2. Relative MP2/6-31+G*/HF/6-31+G* activation free-energy profile for the gas-phase reaction of $(\text{OH})^-$ with MEP (top) and the change in profile upon solvation (bottom). The zero of energy corresponds to the reactants at infinite separation. The numbers correspond to the free-energy differences of subsequent points.

Scheme 3. Schematic Diagram Depicting Fully Optimized HF/6-31+G* Structures for the Reaction of $(\text{OH})^-$ at Phosphorus of MPP (MPP(P)) (Not All Transition States and Intermediates along the Pathways Are Depicted for the Sake of Clarity)

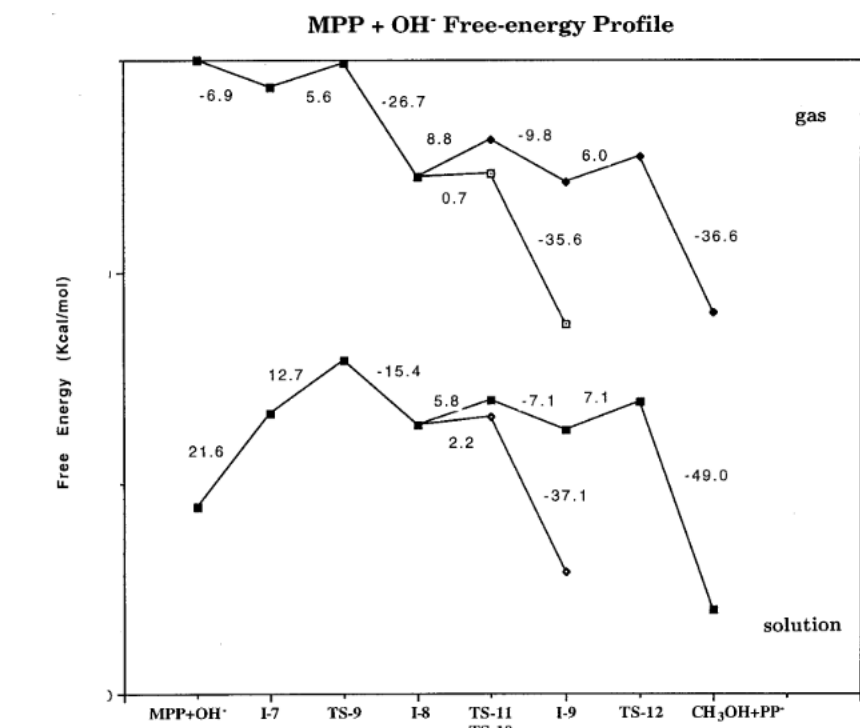
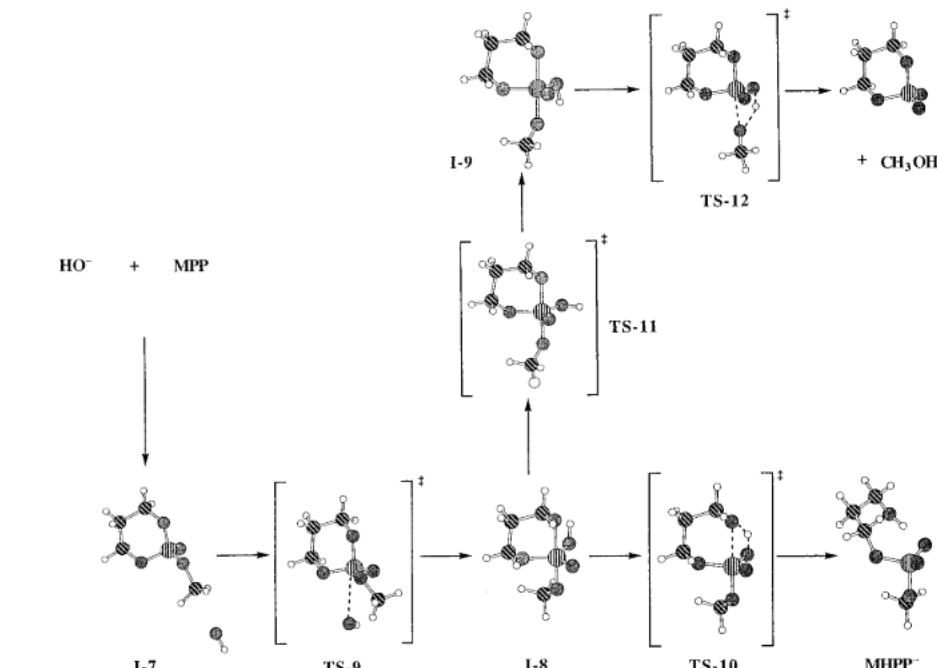


Figure 3. Relative MP2/6-31+G*/HF/6-31+G* activation free-energy profile for the gas-phase reaction of $(\text{OH})^-$ with MPP (top) and the change in profile upon solvation (bottom). The zero of energy corresponds to the reactants at infinite separation. The numbers correspond to the free-energy differences of subsequent points.